Polymeric Molecular Coatings for Oxidation Resistance Property of Metal Surfaces

NGUYEN HAI THANH

2018

Materials and Life Science

Graduate School of Science and Technology

Kyoto Institute of Technology

Contents

Chapter 1

General Introduction

1.1 Metals used in the electrical industry application

Nowadays, in modern society, the daily activities are very closely linked to the use of electricity because many appliances are used in daily life. In the electrical industry, metals are an indispensable resource with a multitude of applications. Metals are important to a high energy society: they transport electricity in the electrical grid, and provide many other services. Many materials are used to transmit electrical energy but those most frequently specified for types of conductors are gold, silver, copper, high strength copper alloys, steel, nickel, and aluminum. The conductive metals have the different level of conductivity – some obviously being better than others (Table 1.1).

Gold - Gold has a highest resists oxidation, but its lower conductivity and more expensive. As a result gold is used to plate connectors, whose connection may degrade if the surface is oxidized.

Silver - Silver has a highest conductivity than all metals, but isn't used widely due to its cost. But it is used in some areas with extremely low resistance, such as in sensitive scientific instruments; and also in the electrical contacts in the switch.

Aluminum - Aluminum has conductivity lower than copper, but it cheaper and lighter than copper. The aluminum wire with the same conductivity as copper wire would be physically thicker, but would still work out to be lighter.

Copper – Copper is the most widely used conductor material. Its physical properties are high electrical and thermal conductivity, ductility, malleability and solder ability, high melting

point. Therefore, copper is an irreplaceable in many fields: from electrical engineering to buildings to computer and integrated circuit manufacture.

Nickel – Nickel has good properties, which include electrical conductivity, magnetic permeability, thermal conductivity, thermal expansion, hardness, strength, formability, and ability to be soldered, brazed or welded. The applications range of nickel is very large from very large electronic pieces to nano-scale technology.

Table 1.1. The physical properties of metals used in the electrical application

Material	Resistivity (Ohm.m, 20 ^{o}C)	Conductivity (Siemens/m)	Thermal Conductivity (W/m.k)	Density (g/cm3)	Melting point $^\circ$C
Silver	1.59×10^{-8}	6.29×10^{7}	427	10,5	961
Copper	1.68×10^{-8}	5.95×10^{7}	401	8,9	1083
Gold	2.35×10^{-8}	4.10×10^{7}	317	19,4	1064
Aluminum	2.65×10^{-8}	3.50×10^{7}	237	2,7	660
Nickel	6.99×10^{-8}	1.43×10^{7}	91	8,8	1455
Iron	9.71×10^{-8}	1.03×10^{7}	80	7,9	1528

Metal oxide – Most of metals are oxidized by oxygen in air. The initial oxidation of a bare metal surface is generally understood to begin with the adsorption of O_2, which subsequently dissociates into adsorbed atomic oxygen [1]. The O atoms then covalently bond to adjacent metal atoms, weakening the attachment of the latter to the metal crystal. This is followed by the place exchange of a metal and an O^{2-} ion at the metal/gas interface resulting in the formation of the first one or two monolayers of oxide.

In the presence of water and oxygen (or simply air), some elements such as copper [2, 3], nickel [4], and iron [5] rapidly oxidize. The surface of most metals becomes oxides and hydroxides in the presence of air. These oxide layer were decreased the electrical conductivity of metal surface. This is big problem in the electrical industry to transform energy

1.2 Oxidation of copper

There are two different mechanisms of copper oxidation. In air at ambient temperature, a thin layer of cuprous oxide (Cu_2O) forms first on the copper surface, and cupric oxide (CuO) is formed slowly only through a second step of oxidation (Figure 1.1) [6]. The reactions involved in the entire synthesis can be summarized as the following.

$$4Cu \quad + \quad O_2 \quad \rightarrow \quad 2\,Cu_2O \tag{1-1}$$

$$2Cu_2O \quad + \quad O_2 \quad \rightarrow 4\,CuO \tag{1-2}$$

Figure 1.1. Growth mechanism for copper oxides.
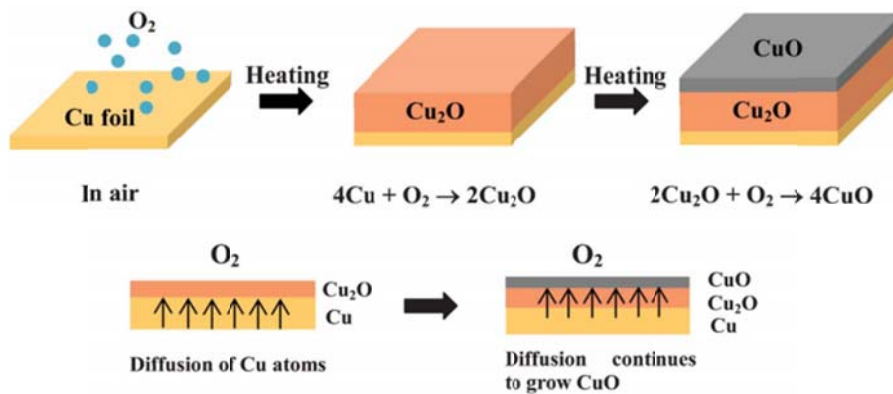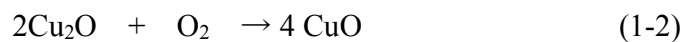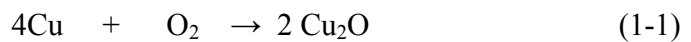
Figure 1.1 shows the oxidation processes of Cu plate heated in air. Cu_2O was first formed at the interface of Cu plate and air, and CuO was formed at the top surface of the Cu_2O layer. The transformation from Cu to Cu_2O is more facile than that from Cu to CuO based on their crystal structures. This oxide layer exhibits electrical insulation of copper surface, so that

the electrical conductivity is impaired by intervening at the contact interface. The progress of copper oxidation is accelerated by temperature rise.

Wieder and Czanderna [7] described the formation of oxide areas on copper surfaces when heated from room temperature to 330°C. They are seen in Figure 1.2 and are classified into different temperature regimes: (1) below 70°C, shown an oxidative growth typical of an amorphous oxide; (2) 70–110°C and (4) 200–270°C, shown abrupt regions of sudden change in the film composition followed by an increase of the thickness; and (5) 270–330°C related to the existence of cupric oxide growth.
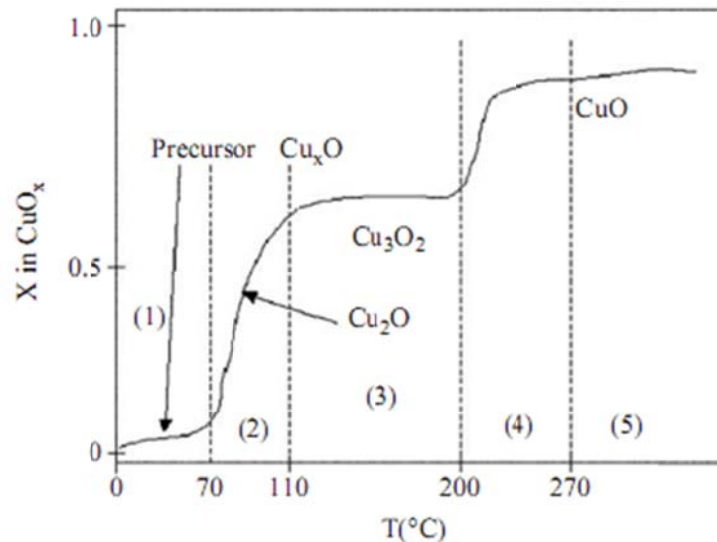
Figure 1.2. Formation of different copper oxides as a function of temperature in a 13.3 kPa atmosphere of oxygen.

Tamai et al. demonstrated that the thin oxide layer formed on the surface in the vicinity of room temperature, but this reaction proceeds greatly as the heat temperature over 100°C in the long heat treatment time [8]. From the contact resistance measurement, they determined that the oxide layer on the copper plate is thin at low temperature. However, at high temperature, the

oxide layer thickness increased rapidly. Since the oxide film formed on the copper surface greatly increases the electrical resistance, it is a big problem of copper in the industry application.

1.3 Oxidation of nickel

The oxidation of Ni surfaces at ambient temperatures was first suggested by Mott and Cabrera [9]. The mechanism demonstrates the formation of nickel oxide on the surface. Reactant O_2 molecules adsorb onto the surface of the metal and decompose into atomic oxygen. The atomic oxygen then bonds covalently with the Ni metal atoms at the surface, weakening their attachment to the lattice. Owing to the difference in electronegativity between Ni and O, a dipole forms which allows the two atoms to exchange places. At higher temperatures, the exposure of Ni metal to O_2 results in the formation of thicker films than those found at lower temperatures. The conversion of nickel that occurs in the oxidation process is expected to follow the reaction:

$$2Ni \quad + \quad O_2 \quad \rightarrow \quad 2\,NiO \quad\quad\quad (1\text{-}3)$$
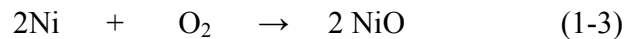
1.4 Metal surface evaluation method

1.4.1 X-ray photoelectron spectroscopy (XPS)

XPS uses soft X-rays to excite core and valence electrons within the atoms of a surface. If the X-ray energy is large enough photoelectrons are expelled from the material and their kinetic energies (KE) are measured by the instrument. This excitation process is known as the photoelectric effect and is illustrated in Figure 1.3. Differences in chemical elements within the near surface region are identified on the basis of their binding energy (BE), which is measured

relative to the Fermi level of the individual atoms. The KE and BE of the photoelectron are related via the following equation (1-4):

$$E_K = h\nu - E_B - \varphi \qquad (1\text{-}4)$$

Where, $h\nu$ represents the energy of the absorbed photon and φ is the work function of the sample. Therefore, when the kinetic energy of electrons is measured from the Fermi level, it becomes as shown in equation (1-5).

$$E_K = h\nu - E_B \qquad (1\text{-}5)$$

The electrons of each element in the sample are bound to the quantized energy level. When a sample is irradiated with soft X-rays with same energy ($h\nu$), the electrons with various kinetic energies are released by photoelectric effect. X-ray photoelectron spectroscopy (XPS) analysis method reveals the information on the elemental composition and chemical state in the sample from the kinetic energy and photoelectron quantity of released photoelectrons.
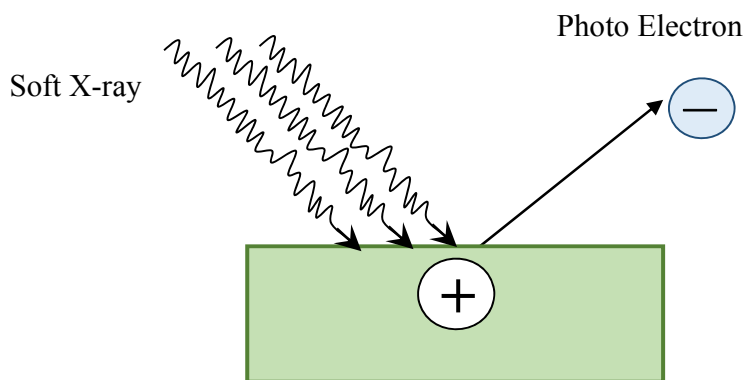

Figure 1.3. A frame format of photoelectron emission by irradiating X-ray.

The energy distribution of the observed electron has information on the inner shell and the valence band of the substance. Therefore, from Equation (1-4), the binding energy E_B can be

obtained with hv. Since the binding energy of each orbital electron differs from element to element, it is possible to easily identify the element by measuring E_K. Also, the bond energy of the same element orbit varies slightly depending on the state and environment around the atom of interest. The state of the element can be analyzed by measuring this change amount.

Also, in order to perform state analysis, we need to find the energy binding of electrons. Therefore, it is necessary to find the work function φ and obtain the measured binding energy from the Fermi level. In the actual measurement, in the case of a metal sample, the Fermi level of the sample matches the Fermi level of the spectrometer, so that the binding energy is expressed by the formula (1-5). The relationship between irradiation X-ray energy, binding energy, and kinetic energy is shown in the formula (1-6).

$$E_B = h\nu - E_K - \varphi_{SP} \tag{1-6}$$

Where, E_B is the coupling energy of electrons based on the Fermi level, and φ_{SP} is the work function of the sample spectrometer.

Since many polymeric materials are insulators, photoelectrons are released during XPS spectrum measurement and the surface is positively charged, and depending on the sample history, it may be already charged before XPS measurement [11-14]. Generally it is difficult to determine accurate binding energy. Therefore, the C_{1s} peak of (-CH2 -) in the polymer is appropriately set to 285.0 eV and used as a standard of binding energy.

1.4.2   Focused ion beam device (FIB)

The focused ion beam (FIB) system is an important tool for understanding and manipulating the structure of materials at the nano-scales [15, 16]. FIB device scans the specimen surface with an extremely thinly focused ion beam, detects secondary electrons generated and observes the microscopic image, and processes the surface of the specimen.

The FIB apparatus has the same configuration and function as SEM, and the only

difference is the use of a gallium ion (Ga $^+$) beam instead of electron beam [17]. The sample observation in this device is basically the same as the scanning electron microscope, and the light generated from the light source is focused by an aperture or a focusing lens (also called a condenser lens, CL) to form a beam, subsequently an objective lens focusing on the sample surface with an objective lens (also called OL). The focused and focused beam on the sample surface is scanned by the deflector surface. Then, the secondary signal generated from the sample surface by the beam irradiation which is detected by the detector, and the data corresponding to the secondary signal is stored in the image data memory corresponding to the beam irradiation position coordinate. By displaying the data stored in the image data memory on the computer screen, it is possible to observe the microscopic image of the region irradiated with the beam. The main functions of the focused ion beam apparatus are roughly divided into "etching" and "deposition".

The gallium ions are much heavier than electrons, a so-called sputtering phenomenon occurs in which atoms constituting a sample are flicked out. The ejected atom becomes secondary ion and jumps out of the specimen. The surface of the sample can be etched by increased the amount of this ion beam and increased amount of atoms sputtered. Thus, it is possible to realize maskless processing for selectively etching only the portion irradiated with the ion beam. By applying this technique, we can possible to perform cross-section processing observation in which a predetermined portion of a sample is etched and the cross-section is exposed and observed, and furthermore, a TEM sample making processing for taking out a predetermined portion of the sample as a flake can be performed.

Figure 1.4 shown the compound gas can be locally deposited by blowing the compound gas near the ion beam irradiation region on the sample surface. When the sample irradiated with

primary ions, secondary electrons generated, and the secondary electrons contribute to decomposition of the compound gas and the compound gas separated into a gas component and a solid component. The gas component evacuated but the solid component deposited on the sample surface. As a result, deposition can be selectively performed in the ion beam irradiation region with no mask.
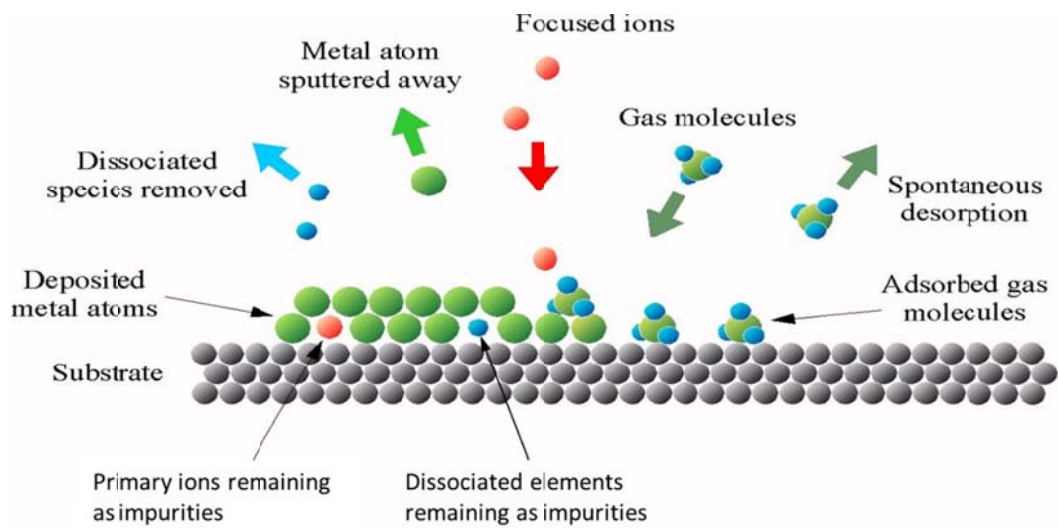

Figure 1.4. Principle of deposition treatment by FIB.

The FIB provides huge advantages to the preparation of specimens for microscopy analysis including SEM, transmission electron spectroscopy (TEM), and other characterization techniques [18, 19].

1.4.3 *Scanning transmission electron microscope (STEM)*

Scanning transmission electron microscopy (STEM) techniques are indispensable for characterizing interfaces and defects, nano−devices, nanoparticles and catalysts, and other nano−systems [20]. The single most important feature of a STEM instrument is its versatility: atomic resolution images, diffraction patterns from nanometer regions and nanometer-scale spectroscopy data can be obtained either simultaneously or sequentially from the same region of

the specimen.

When an electron nanoprobe interacts with a specimen inside a STEM instrument, a variety of electron, electro-magnetic and other signals can be generated. Figure 1.5 shows a schematic diagram illustrating the common signals that are used in a dedicated STEM instrument. All these signals can be used to form images or diffraction patterns of the specimen or can be analyzed to provide spectroscopic information.
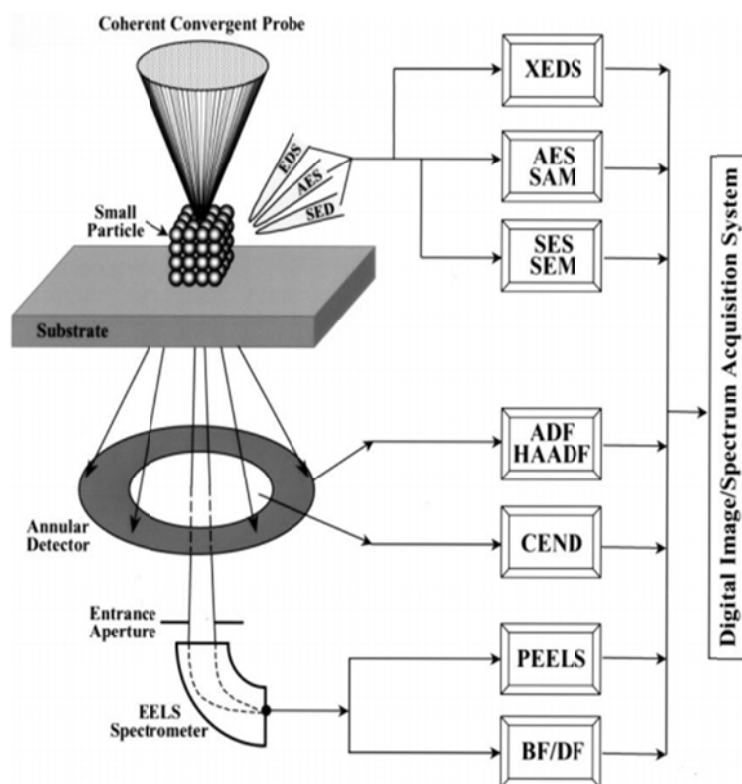

Figure 1.5. Schematic diagram illustrates the various signals generated inside a scanning transmission electron microscope that can be used to form high-resolution images, nano−diffraction patterns or spectra of the region-of-interest.

1.4.4 Electrochemical technique

Linear potential sweep is a potentiostatic technique [21], in the sense that the potential is the externally control parameter. The potential is changed at a constant rate:

$$v \quad = \quad \frac{dE}{dt} \qquad (1\text{-}7)$$

and the resulting current is followed as a function of time.

In most case the potential is swept forward and backward between two fixed values, a technique referred to as cyclic voltammetry (CV). In this way the current measured at a particular potential on the anodic swept (going from negative to positive potential) can readily be compare with that measured at the same potential on the cathodic swept (going from positive to negative potential). A typical CV is shown in Figure 1.6 [22].
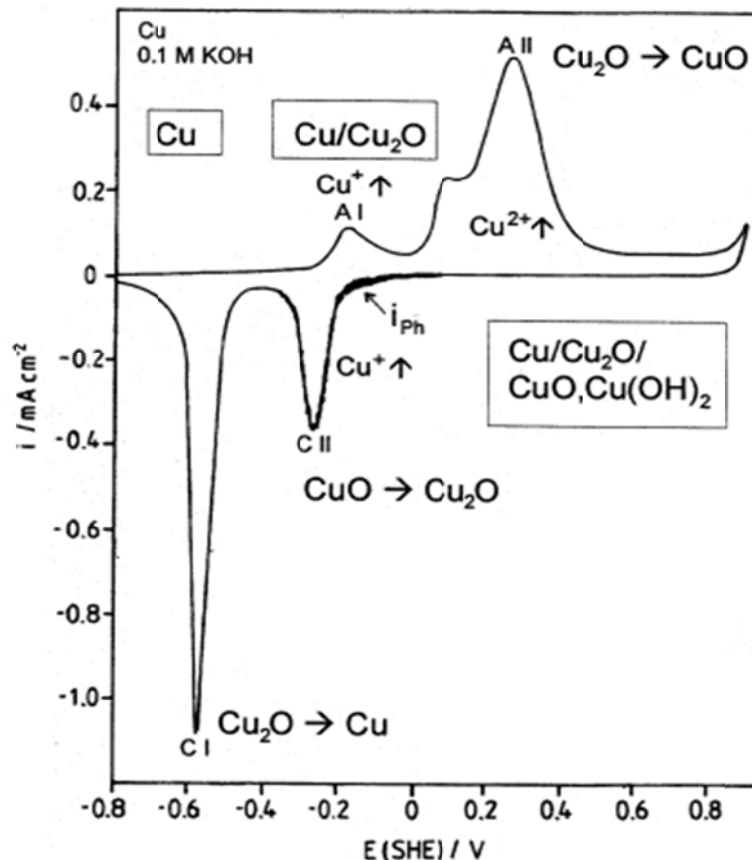

Figure 1.6. Potentiodynamic polarization curve of Cu in 0.1 M KOH with dE/dt=10 mV s^{-1} with

indication of peak potentials of layer formation (AI, AII) and reduction (CI, CII) and dissolution of Cu-ions and stability range of anodic oxide layers, irradiation with chopped light causes current oscillation due to superimposed photocurrent i_{Ph} at peak CII [22].

Linear potential sweep measurements are generally of three types:

1) Very slow sweeps (in the range of sweep rate about 0.1-5 mVs^{-1}): The sweep rate plays no role in this case, except that it must be slow enough to ensure that the reaction is effectively at steady state along the course of the sweep. Reversing the direction of the sweep should have no effect on the current potential relationship, if the sweep is slow enough. Deviation occur sometime as a result of slow formation and reduction of surface oxides or passive layers. Because the sweep rate too slow, the potential is often swept only in one direction, and the experiment is then referred to as linear sweep voltammetry (LSV).

2) Studies of oxidation or reduction of species in the bulk of the solution. In this case, the sweep rate is usually in the range of 0.01 – 10 Vs^{-1}. The lower limit is determined by the need to maintain the total time of the experiment below 10 - 50 s. The upper limit is determined by the double layer charging current ad by the uncompensated solution resistance.

3) Studies of oxidation or reduction of species adsorbed on the surface. The redox behavior of species that are adsorbed on the surface is usually activation controlled and influenced by the remaining number of the free site on the surface. The sweep rate also in the range of 0.01 – 10 Vs^{-1}, but here the lower limit is determined by background currents from residual impurities in solution, white upper limit is determined by the uncompensated

solution resistance and by instrumentation.

In this study, linear sweep voltammetry was used as an electrochemical evaluation of the metal surface on which an organic thin film had been formed in addition to the above CV measurement. Metals (Cu and Ni), Pt, and Ag / AgCl electrode were used for the working electrode, counter electrode and reference electrode, respectively. Metal oxide on the surface was cathodically reduced by LSV measurement and the oxidation resistance of the nickel surface was quantitatively evaluated from the reduced charge amount.

1.4.5 Electrical conductivity

Electricity is the most important part of modern everyday life. It is used to run product machinery, transportation, communications, medical procedures, military operations, research, and so on [23-25]. Since the beginning of the 19th century, electricity has been studied and applied by many scientists.

Electric charge – Elementary quantity of charge is ± 1e, with the electron carrying a charge of -1e and the proton +1e. The unit of charge is 1C (coulomb).

Voltage – The fundamental definition of voltage relates to the work required to move a unit charge between two points. By the definition, the unit of charge is positive. The amount of work does not require a reference level. The work required is measured by the potential difference. It is correct to say the work per unit charge is the voltage difference. The unit of voltage is a volt (V).

Electric currents – Electric current is the charge passing through a given cross section of the conductor per unit time. Electrons are carriers of the charge. If the charge dq passes through a hypothetical plane in time dt, then the current through that plane is

$$i \quad = \quad \frac{dq}{dt} \qquad\qquad (1\text{-}8)$$

The SI unit for current is the ampere (A). That is, 1 ampere = 1 coulomb per second.

Current is a scalar. If a current splits in to branches, the magnitude of the partial currents must add to yield the magnitude of the current in the original conductor (i_0). For example, for two branches (Figure 1.7), this can be expressed as

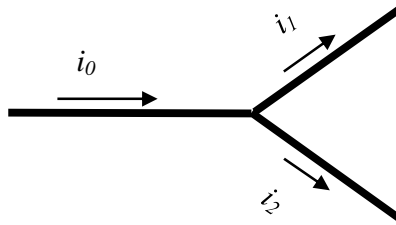$$i_0 \quad = \quad i_1 + i_2 \tag{1-9}$$

Figure 1.7. Current splitting at a junction into two branches.

Ohm's law – Ohm's law is valid for circuits, expresses the relationship between current, voltage, and resistance.

$$E = I * R \tag{1-10}$$

where E = potential (in V); I = current (in A); and R = resistance (in Ω).

Resistance– The electrical resistance of the conductor is a function of its length (L) and the conductor area (A). Ohm's law tells us that for a given resistance (R), the current flowing through the conductor is proportional to the applied voltage.

$$R \quad = \quad \frac{V}{i} \tag{1-11}$$

The SI unit for resistance is the ohm (Ω).

Resistivity - The electrical resistivity of conductor material is a measure of how strongly the material opposes the flow of electric current through it. This resistivity factor enables the

resistance of different types of conductors to be compared to one another at a specified temperature according to their physical properties without regards to their lengths of cross-sectional areas. The resistivity of the material is defined as:

$$\rho \;=\; \frac{E}{J} \tag{1-12}$$

where, E - the electric field at a point in a resistive material instead on the potential difference V across a particular resistor. J – The current density at the point in question instead of the current through the resistor. The unit of resistivity is ohm-meter (Ωm).

Conductivity – The reciprocal of the resistivity of a material is its conductivity, defined as:

$$\sigma \;=\; \frac{1}{\rho} \tag{1-13}$$

The SI unit of conductivity is siemens (S).

Electrical resistance measurement – Electrical conductivity is an important experiment tool to probe electrical transmission of metallic materials and semiconductors. In the room temperature environment, the electrical resistance measurement usually measured by connecting two terminals to both ends of the sample to be measured by using a multimeter. The small diameter cable connected to the specimen, which used for the purpose of suppressing the inflow of heat transmitted through in this cable. In this case, if the object to be measured is a superconductor, the electric resistance to be measured becomes infinitely small, the electric resistance and the contact resistance of the metal cable becomes a non-negligible value.

In the two-terminal measurement method, the resistance of the wiring for measurement included measurement error, however, the contact resistance of the component connected to the sample can be avoided by using the four terminal method.

1.4 Survey of this thesis

In this thesis, I investigated the influence of polymeric molecular coatings on the electrical and air oxidation resistance properties, and electrical conductivities of metal surfaces. Chapter 1 discusses the background and purpose, importance and related research of this research. In chapter 2, molecular coatings of thiol terminated organic compounds such as thiol terminated polystyrenes and alkanethiols were examined on the nickel surfaces by means of interaction between nickel and thiol groups in order to investigate air oxidation resistance properties of the surface by the coatings. Conductivity measurements, CV, and LSV measurements were carried out for the organically modified nickel surfaces in order to characterize qualitative and quantitative oxidation resistance properties of the surfaces. The results indicate that the thiol terminated polystyrene provides higher heat resistance property than alkane thiols with maintaining electrical conductivity. In chapter 3, investigation of molecular weight of polystyrene molecular coating on the oxidation resistance property of the modified copper surface was examined. It was observed that the higher thermal stability was supplied by longer chain of the polymeric coating. The results of quantitative analyses by electrochemical approach indicate that the higher air oxidation resistance property was provided by longer polymer chain of the coating, whereas shorter chain gave higher electrochemical oxidation resistance properties on the surface. In chapter 4, the researches were summarized. The future

prospects of the polymeric molecular coatings were also described.

References and Notes

1. Jacques Benard, The oxidation of metal and alloys (1964)

2. C. G. Cruzan, H. A. Miley, J. Appl. Phys. 1940, 11, 631.

3. D.L. Cocke, R. Schennach, M.A. Hossain, D.E. Mencer, H. McWhinney, J.R. Pargae, M. Kesmez, J.A.G. Gomes, and M.Y.A. Mollah, Vacuum 79 (2005) 71–83.

4. Brad P. Payne, Andrew.P.Grosvenor, Mark C. Biesinger, Brad A. Kobe and N. Stewart McIntyre, Surf. Interface Anal. 2007; 39: 582–592.

5. Frederic E. Schubert, J. Chem. Educ. 2015, 92, 517−520.

6. K. Chen, S. Song, D. Xue, Cryst. Eng. Commun. 2013, 15, 144.

7. Harold Wieder, and A. W. Czanderna Journal of Applied Physics 37, 184 (1966)

8. T. Tamai, T. Kawano, IEICE Trans. Electron. 1994, 10, 1614.

9. B.P. Payne, M.C. Biesinger, N.S. McIntyre, Journal of Electron Spectroscopy and Related Phenomena 175 (2009) 55–65.

10. Cabrera N, Mott NF. Rep. Prog. Phys. 1948–1949; 12: 163.

11. Lili Zhu, Xiaoliang Wang, Qiang Gu, Wei Chen, Pingchuan Sun, and Gi Xue, Macromolecules, 46 (6), 2292 (2013).

12. J. Christopher Love, Lara A. Estroff,Jennah K. Kriebel, Ralph G. Nuzzo, and George M. Whitesides, Chem. Rev. 2005, 105, 1103−1169.

13. Bain, C. D.; Whitesides, G. M. J . Phys. Chem. 1989, 93, 1670- 1673.

14. Bain, C. D.: Troughton, E. B.: Tao, Y.-T.; Evall, J.; Whitesides, G. M.; Nuzzo, R. G. J. Am. Chem. Soc,. 1989, 111, l2l 335.

15. Walker, J.F., Reiner, J.C., Solenthaler, C. Proc. Microscop Semiconductor Material Conf., Oxford (1995).

16. Kim, C.S., Ahn, S.H., Jang, D.Y. Vacuum 86 (8), 1014–1035 (2012).

17. Volkert, C., Minor, A., Mrs Bull 32 (5), 389–395 (2007).

18. Reyntjens, S., Puers, R. J. Micromech. Microeng. 11 (287), 300 (2001).

19. Giannuzzi, Lucille, A., Stevie, F.A. Springer (2005).

20. Jingyue Liu, Journal of Electron Microscopy 54(3), 251–278 (2005).

21. Eliezer Gileadi, Physical Electrochemistry: Fundamentals, Technique and Application (2011) 15, 221.

22. U. Collisi, H.-H. Strehblow, J. Electroanal. Chem. 210(1986) 213.

23. Jiri George Drobny, Polymers for electricity and electronics: Materials, Properties, and Appliacions (2011).

24. N. F. Mott, 6 Proc. Phys. Soc.,' vol. 47, p. 571 (1935), referr

25. John Bardeen, Journal of Applied Physics 11, 88 (1940).

26. F. Yakuphanoglu et al. Physica B 334 (2003) 443–450.

Chapter 2

Polymeric molecular coating on oxidation resistance property
of nickel surface

2.1 Introduction

Nickel is widely used in industry for platting, electro-forming, and producing alloys. Those nickel derivatives as well as neat nickel metal are useful as electrically conducting materials due to their practical properties, for instance, electrical conductivity, ductility, low cost, and process ability. They are known to easily react with oxygen in air, and form metal oxides on the surface [1-3]. Since the metal oxides are normally electrical insulators, surface conductivity significantly drops by oxidation. In order to prevent oxidation, those surfaces are usually coated with oxidation inhibitors or inert metals. These methods still have problems with the high cost of the coatings and inhibition of surface conductivity. An approach for introduction of oxidation resistance on copper surfaces was recently developed while retaining high conductivity of the surface by means of molecular coatings with low-molecular-weight thiol compound and thiol-terminated polymers [4,5] by using thiol-copper interaction. Oxidation resistance and electrical conductivity on the metal surfaces were investigated by X-ray photoelectron spectroscopy (XPS) [6-13] and cyclic voltammetry (CV). [14-16]

Since oxidation of nickel surfaces is a problem for electrical usage, here in this chapter, surface modifications with thiol-terminated organic compounds [17-23] were examined on nickel surface for electrical applications. The modified surfaces are electrically characterized as well as with XPS analysis [22] to investigate the effect of the organic coatings on oxidation resistance properties.

2.2 Experiment

2.2.1 Materials

s-BuLi (1M solution in hexane) was purchased from Kanto Chemical. Styrene (Wako Pure Chemical, 99%) was distilled twice over CaH2 under reduced pressure and sealed in ampule with a breakable seal. 1-Dodecanethiol (Nacalai Tesque, Inc. 95%) was distilled before use. Ethanol (Wako Pure Chemical, 99.5%) and toluene (Nacalai Tesque, Inc. 99%) were distilled and degassed by N2 bubbling before use. Nickel plates were purchased from Nilaco. Other reagents were used as supplied. Thiol terminated polystyrene was synthesized by anionic polymerization of styrene with ethylene sulfide as a terminating agent under high-vacuum in a sealed reactor.

2.2.2 Modification of nickel surface

Nickel plates were polished by means of polishing paper (#1000, #2000, #4000, and #8000) and electric polishment. After polishing, the plates were washed with water, and subsequently sonicated in toluene and methanol. The plates were dried under vacuum. Before surface modification, metal oxide on the nickel surface was removed by dipping of specimens in 3.7 % HCl-ethanol solution for 5 min. The plates were subsequently rinsed with distilled ethanol and dried under vacuum for 20 min.

To allow the deposition of thiol derivatives, the nickel plates were dipped in toluene solution of thiol terminated polystyrene or ethanol solution of 1-dodecanethiol, for 20 hours at 35°C. After making coatings of organic compounds on the nickel surface, the specimens were rinsed with the respective solvents to remove excessive organic compounds, and dried under vacuum for 20 min (as shown in Figure 2.1). The schematic diagram of the thiol compound chemically adsorbed on nickel surface was shown in Figure 2.2.
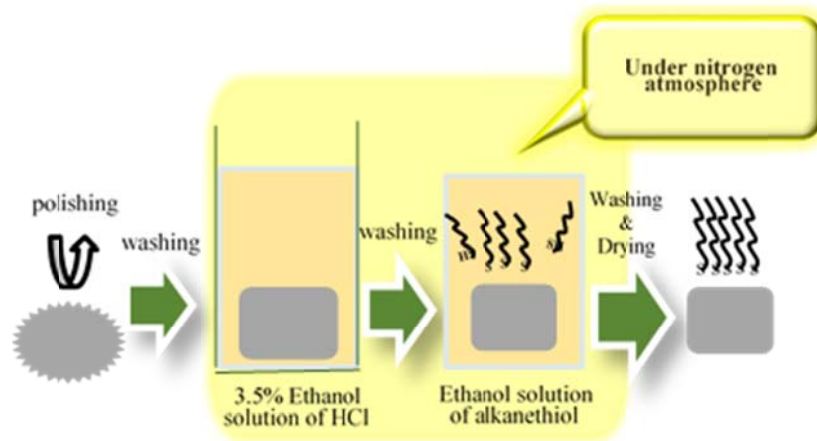
Figure 2.1. Scheme of the process of making thin layers of thiol terminated organic compounds.
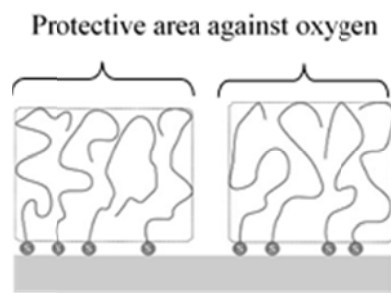

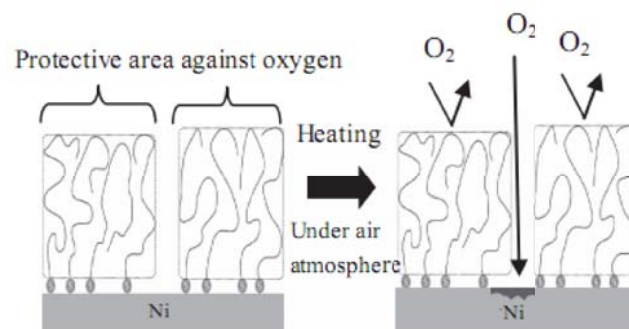**Figure 2.2.** Schematic image of nickel covered with thiol terminated polymer.

Figure 2.3. Oxidation resistance property of nickel surface with molecular coating of PSt-SH.

2.2.3 Measurements

^{1}H-NMR spectrum was recorded at 25°C on a Bruker DPX-400 spectrometer in CDCl$_3$. Gel permeation chromatography (GPC) was performed at 25°C with TSK gel G5000HHR and G3000HHR on TOSOH HLC-8320 by using chloroform as an eluent after calibration with standard polystyrenes.

XPS measurements were carried out on JEOL JPS-9010MC. Photoelectron spectra of S$_{2p3/2}$ were investigated in the binding energy range between 159 and 169 eV.

CV and LSV were carried out on ECstat-300 (EC FRONTIER, Japan). Pt was used for counter electrode, and Ag/AgCl was used for reference electrode. CV was measured with sweeping voltage range from -600 mV to 600 mV with a rate at 1000 mV/s in 0.1M NaOH aq under N$_2$ flow at 50 mL/min (Table 2.1). LSV was measured with sweeping voltage range from 600 mV to -600 mV with a rate at 1000 mV/s in 0.1M NaOH aq under N$_2$ flow at 50 mL/min. Electrical resistance of copper plates was determined by contact electric resistance measurement. For measurement of contact electric resistance, electrical conductivity was evaluated by applying a contact type four terminal method. It was confirmed that there was almost no change in electrical conductivity with respect to a change in distance between the two probes. In this case, contact was made at an interval of 2 cm, and measurement was made under the condition of plane to semispherical surface (Au plating probe, curvature radius 30 μm). Measurement was carried out by connecting a measuring instrument and a potentiostat as shown in Figure 2.4.

Table 2.1. Typical experimental condition for cyclic voltammetry

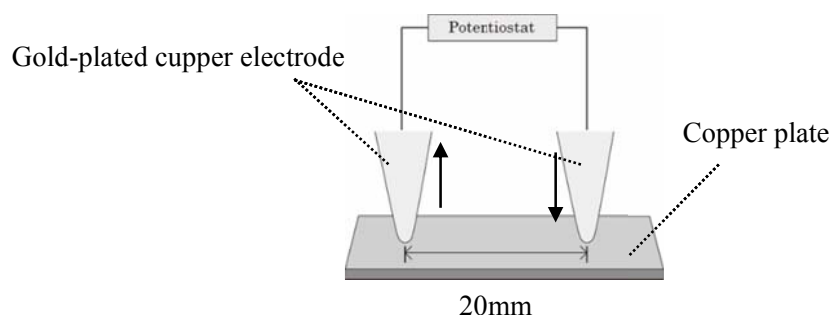| Solution (mL)	Sampling interval (ms)	Filter (Hz)	Sweep rate (mV/s)	Nitrogen gas flow rate (mL/min)
10	1000	10	10	50

Figure 2.4. The apparatus used to measure the contact electrical resistance for the plate specimens.

2.3 Results and discussion

2.3.1. XPS measurement

Two kinds of thiol derivatives, 1-dodecanethiol and thiol-terminated polystyrene ($M_n = 2600$, $M_w/M_n = 1.44$), were applied for surface modification in order to evaluate the effect of molecular weight of the molecular coatings. Three samples, 1-dodecanethiol-deposited nickel (Ni-D), thiol-terminated PSt-deposited nickel (Ni-PSt2600), and unmodified nickel (Ni-bare) were prepared. Depositions of the organic coatings on the nickel plate were confirmed by XPS analysis as shown in Figure 2.5.
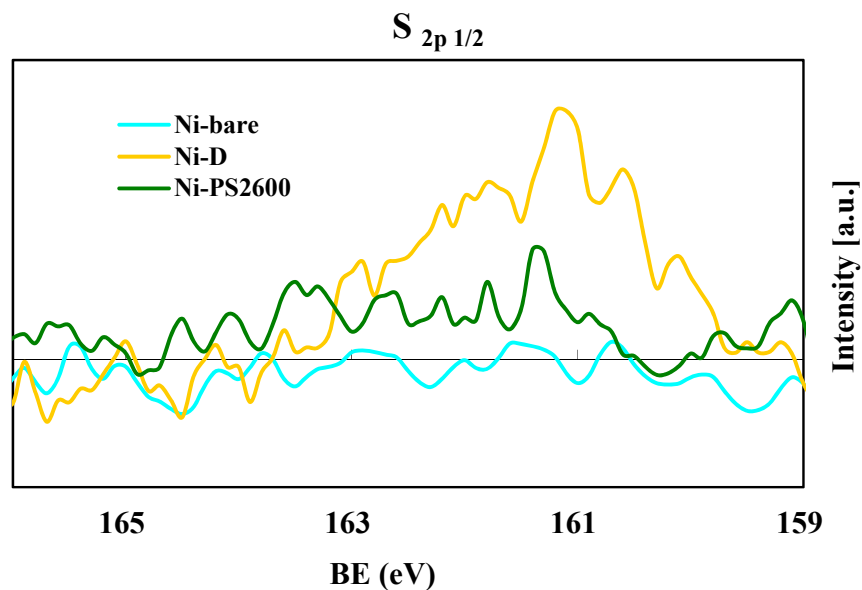
S $_{2p\ 1/2}$

Legend:
- Ni-bare
- Ni-D
- Ni-PS2600

Intensity [a.u.]

BE (eV)

Figure 2.5. Narrow scan photoelectron spectra of $S_{2p\frac{1}{2}}$ on bare nickel and nickel surface modified with SH-PSt and 1-dodencanthiol.

Figure 2.5 shows the photoelectron spectra of $S_{2p1/2}$ on the three samples. In the spectrum of Ni-D, a peak derived from thiol was observed at 159-163 eV, whereas no significant peak was observed in this region in the spectrum of Ni-bare. The results indicate the deposition of 1-dodecanethiol on the nickel surface. In the case of Ni-PSt2600, small peak of $S_{2p1/2}$ derived from thiol group was observed as the case on copper surface, which is due to long polystyrene chain covered over SH groups adsorbed on the nickel surface.

2.3.2. Anodic oxidation resistance of nickel surface

The electrochemical properties of nickel bare and thiol-treated nickel surfaces were determine by CV. This method consisted of electrochemical oxidation and reduction of the unmodified part remaining on the metal surface by sweeping voltage. The voltage was swept from - 600 to 600mV, followed by the reduction to - 600mV.
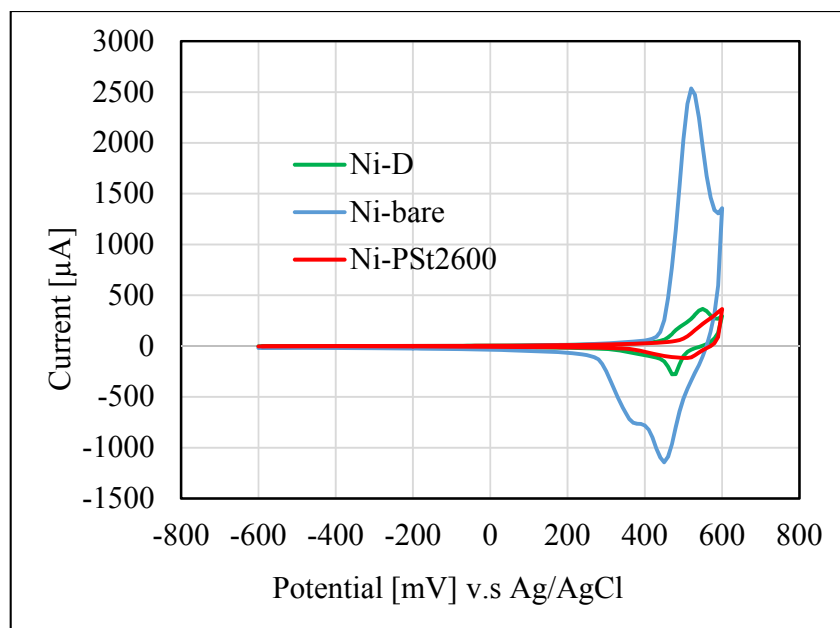
Figure 2.6. Cyclic voltammograms of bare nickel and nickel surface modified with 1-
Dodecanethiol and PSt2600

Figure 2.6 shows the cyclic voltammograms of three samples, which show oxidation and reduction peaks of the surfaces. The electrical oxidation of the nickel surface was carried out from 500 to 600mV to form NiO and Ni(OH)$_2$, and the electrical reduction of the surface to metallic nickel was carried out from 600 to 100mV.

In the voltammograms, the peak area of Ni-bare was large whereas only small peak area was observed for Ni-PS2600 and Ni-D. The peak area indicates the electrical charge for oxidation and reduction of the unmodified area. Hence, the results indicate that the thiol compounds are successfully adsorbed on the surface, and the organic compounds prevent the nickel surface from electrical oxidation in electrolyte. Note that the results do not represent the actual coverage density; however, represent electrical oxidation resistance properties of the organic coatings. Thus, the results of the voltammograms, in which both the peak area of Ni-

PSt2600 and Ni-D are similar size, indicate that resistance of 1-dodecanethiol and polystyrene is similar to electrical oxidation on the nickel surface.

2.3.3 Oxidation resistance of nickel surface coated with thiol compound heat treatment in air

Quantitative air oxidation resistant properties of the nickel surfaces were evaluated by LSV. In this study, LSV was performed on the air oxidized surface from 600 to -600mV in order to measure the electrical charge for reduction of oxide layer. Thus, the surface-modified nickel samples were oxidized by heat treatment at appropriate temperature, and subsequently the oxide on the nickel surface were electrochemically reduced. Figure 2.7-2.10 shows the LSV measurement results of Ni-bare and Ni covered with thiol compounds after heat treatment at 60°C, 150°C, 240°C and 270°C, respectively.
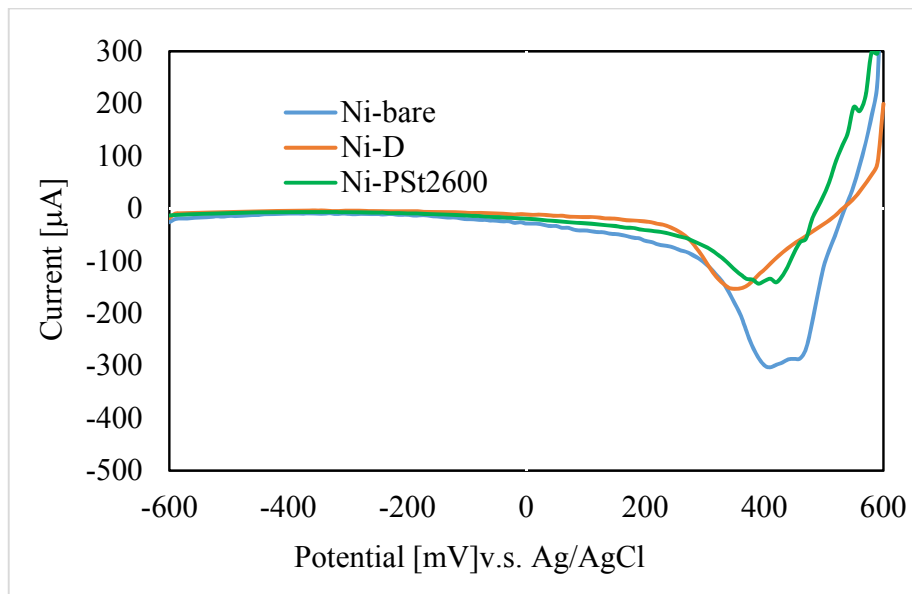

Figure 2.7. LSV voltammograms of bare nickel and nickel surfaces modified with 1-Dodecanethiol and PSt2600 after heating at 60°C.
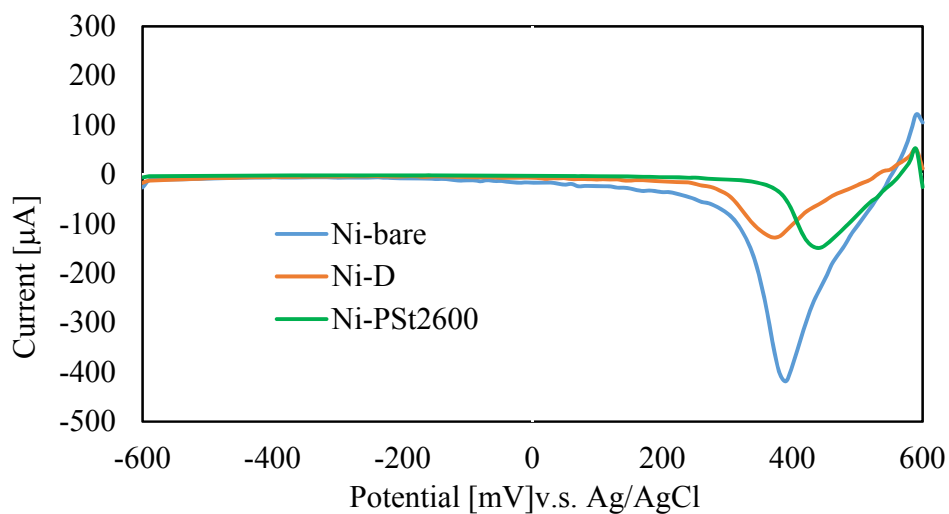
Figure 2.8. LSV voltammograms of bare nickel and nickel surfaces modified with 1-Dodecanethiol and PSt2600 after heating at 150°C.
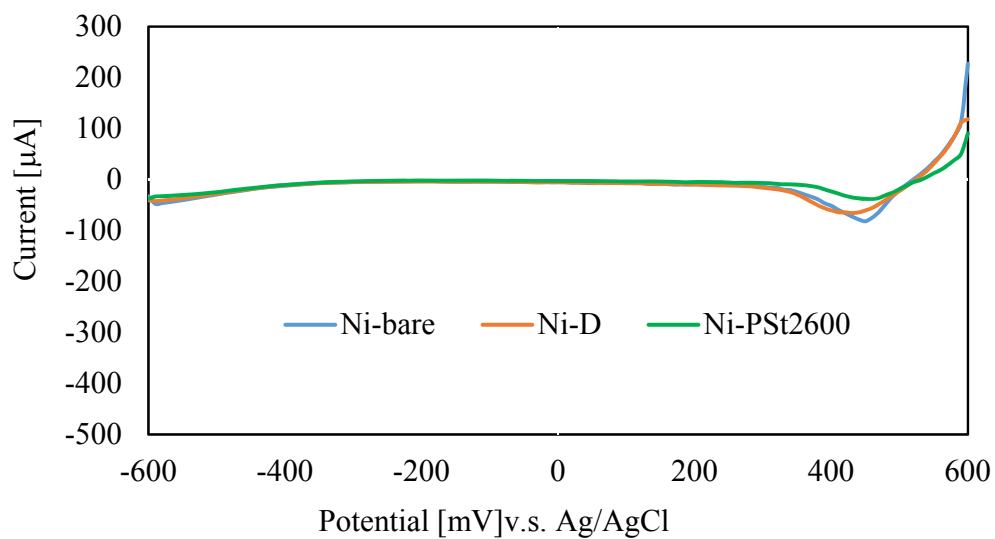

Figure 2.9. LSV voltammograms of bare nickel and nickel surfaces modified with 1-Dodecanethiol and PSt2600 after heating at 240°C.
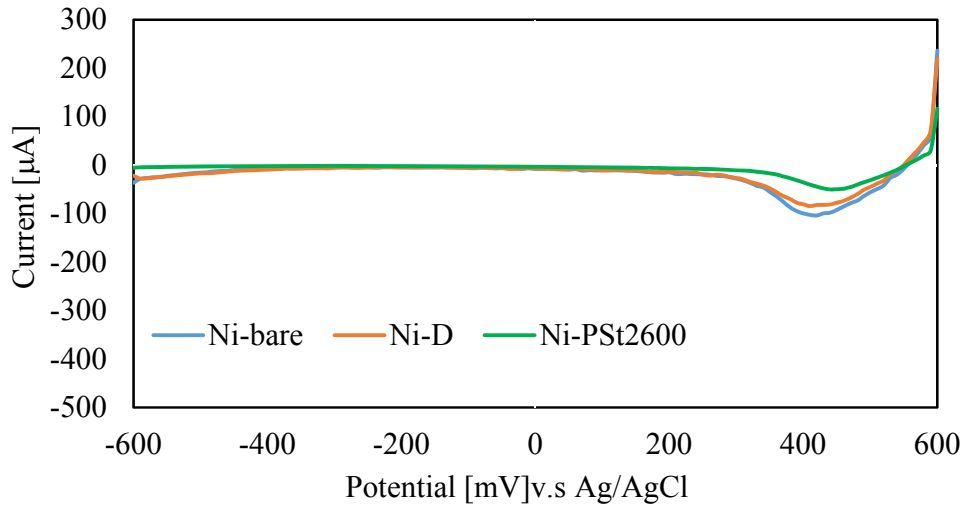
Figure 2.10. LSV voltammograms of bare nickel and nickel surfaces modified with 1-Dodecanethiol and PSt2600 after heating at 270°C.

As shown in Figure 2.7-2.10, at each temperature, the peaks showing reduction in the cathode region decreased when the organic thin film was formed on the nickel surface. The results were considered that the organic thin film on the Ni surface suppressed the formation of the oxide film. However, all of the samples subjected to the heat treatment at 240°C and 270°C, which are high temperature regions, the oxidation amount was smaller than the sample subjected to the low temperature heat treatment. It is considered that this is because a dense oxide film is formed on the nickel surface by heating at a high temperature, and oxygen cannot penetrate into the Ni as the oxide film works as a protective film.

From the above LSV measurement results, the ratios of reduction electric charge for the samples were calculated by the following formula (3-1).

$$\textbf{\textit{Ratio of reduction electric charge}} = \frac{Reduction\ Electric\ Charge(MN)}{Reduction\ Electric\ Charge(UN)} \times 100\ (\%) \quad (3\text{-}1)$$

$$\begin{pmatrix} MN = Modified\ nickel \\ UN = Unmodified\ nickel \end{pmatrix}$$

28

The electric charges for reduction of the oxide on the nickel surfaces are shown in Table 2.2, and the ratios of the charge to that for Ni-bare were calculated (Figure 2.11).

Table 2.2. Electric charge to reduce oxide layer on nickel surfaces after heating at various temperature.

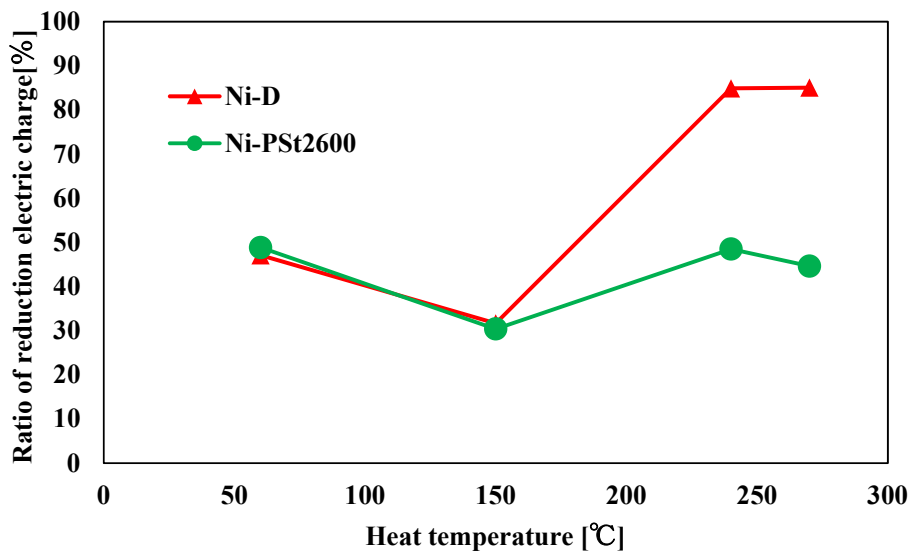| Heat temperature/°C	Electrical charge/mC			
	60	150	240	270
Ni -bare	5.994	5.728	1.06	1.803
Ni-D	2.823	1.813	0.9	1.534
Ni-PSt2600	2.929	1.742	0.514	0.805

Figure 2.11. Ratio of electric charge for reduction of nickel surfaces to that for Ni-bare after heating at various temperatures.

From these results, even after low temperature heat treatment at 60 °C, Ni-bare was oxidized while maintaining electrical conductivity. The result might be due to the complicated oxidation mechanism of nickel surface and the formation of partially oxidized surface. Interestingly, both of the organic-modified samples showed smaller electric charge than Ni-bare at lower temperature (<240 °C), which indicates the barrier effect of the organic layer from oxidation. This barrier effect was observed in Ni-PSt2600 even at high temperature (≥240 °C), whereas Ni-D showed similar electric charge to Ni-bare which might be caused by desorption of 1-dodecanethiol. The results agree with the conductivity measurements in the next section. From these results, we can estimate obvious contribution of long polymer chain to oxidation resistance.

2.3.4 Electrical conductivity of nickel surface coated with thiol compound

Air oxidation resistance of the metal surface covered with the organic coatings and thermal stability of the coatings were investigated by surface conductivity measurements of the samples by four-terminal methods after heat treatment at various temperature in the range of 35-270 °C for 1 h in air. Heating under air promotes oxidation of nickel surface, which increase electrical resistance on the surface. The resistance was plotted with heat treatment temperature in Figure 2.12.
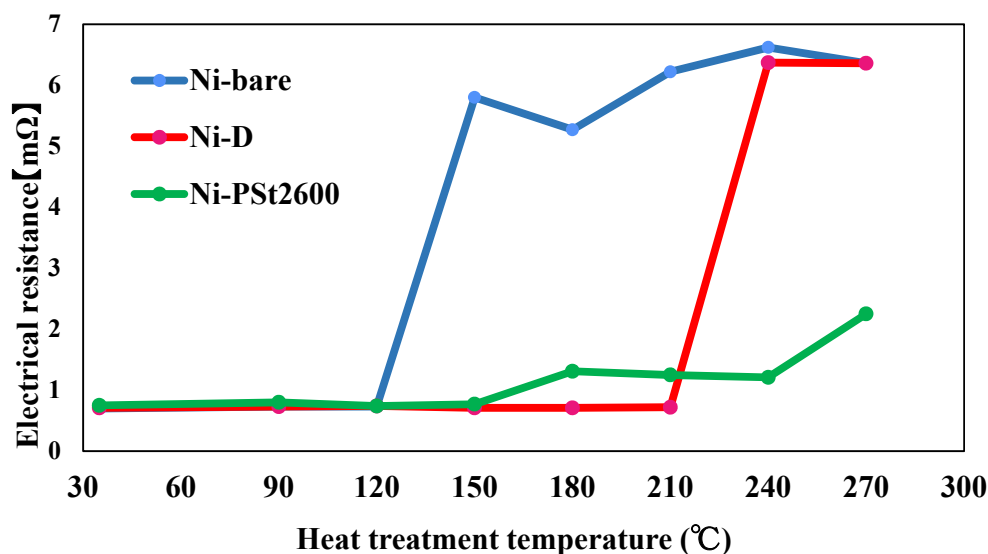
Figure 2.12. Electrical resistances of Ni-bare and Ni-D and Ni-PSt2600 at various temperature.

After heat treatment below 150 °C, all the samples showed low resistance. Thick organic layers may insulate electrical conductivity; however, the low electrical resistances of the samples indicate the organic layers on the nickel surface are thin enough for an electrical junction. The resistance of Ni-bare surface dramatically increased after heat treatment at 150 °C, whereas Ni-D and Ni-PSt2600 retained conductive. These results indicate the organic layers worked as barriers for protection of the nickel surface from oxidation at elevated temperature in the air. In the case of Ni-D, the resistance dramatically increased after heat treatment at 240 °C. Cleavage of Ni-S bonding and desorption of the organic compound were expected above this temperature. Note that the boiling point of dodecanethiol is ca. 270 °C. However, polystyrene-modified surface maintains low electrical resistance even after heat treatment at 270 °C. This can be ascribed to the non-volatility of polystyrene because of long polymer chains, which resulted in oxidation resistance even at such high temperature.

31

2.4 Summary

The organic coatings on the nickel surface by using thiol compounds were performed to prevent oxidation. Cyclic voltammograms of the organic-modified nickel surfaces showed oxidation resistance properties of nickel surfaces by the organic layer from the quantity of the electrical charge during surface electrical oxidation.

Thermal stability of the organic coatings was investigated from surface conductivity measurements and LSV, which showed high oxidation resistance of organic-modified nickel. Interestingly, polystyrene-modified surfaces showed oxidation resistant up to 270 °C while keeping electrical conductivity. Therefore, this approach is applicable for oxidation resistant coatings for electrical devices.

References and Notes

1. T. Tamai, T. Kawano, IEICE Trans. Electron. 1994, E77-C,1614.

2. S. Yokoyama, H. Takahashi, T. Itoh, K. Motomiya, K. Tohji, J. Phys. Chem. Solids 2014, 75, 68.

3. T. Homma, Shinku 1973, 16, 392.

4. T. Ikeda, K. Adachi, Y. Tsukahara, J. MMIJ 2016, 132,39.

5. J. Takagi, T. Ikeda, K. Adachi, Y. Tsukahara, Kobunshi Ronbunshu 2016, 73, 294.

6. M. Watanabe, H. Ando, T. Handa, T. Ichino, N. Kuwaki, Zairyo-to-Kankyo 2007, 56,10.

7. M.-C. Bourg, A. Badia, R. B. Lennox, J. Phys. Chem. B 2000, 104, 6562.

8. X. Mu, A. Gao, D.Wang, P. Yang, Langmuir 2015, 31, 2922.

9. S. Jeong, K. Woo, D. Kim, S. Lim, J. S. Kim, H. Shin, Y. Xia, J. Moon, Adv. Funct. Mater. 2008, 18, 679.

10. S. Tatay, C. Barraud, M. Galbiati, P. Seneor, R. Mattana, K. Bouzehouane, C. Deranlot, E. Jacquet, A. Forment-Aliaga, P. Jegou, A. Fert, F. Petroff, ACS Nano 2012, 6, 8753.

11. R. Sfez, L. De-Zhong, I. Turyan, D. Mandler, S. Yitzchaik, Langmuir 2001, 17, 2556.

12. Y. Lin, O. Ourdjini,L.Giovanelli,S.Clair, T. Faury, Y. Ksari, J. M. Themlin, L. Porte, M. Abel, J. Phys. Chem. C 2013, 117, 9895.

13. P. E. Laibinis, G. M. Whitesides, J. Am. Chem. Soc. 1992, 114, 9022.

14. P. Morf,F.Raimondi, H.-G. Nothofer, B. Schnyder, A. Yasuda, J. M. Wessels, T. A. Jung, Langmuir 2006, 22, 658.

15. S. Yokoyama, H. Takahashi, T. Itoh, K. Motomiya, K. Tohji, Appl. Surf.Sci. 2013, 264, 664.

16. B. C. Worley,W.A.Ricks, M. P. Prendergast, B. W. Gregory, R. Collins, J. J. Cassimus, Jr.,

R. G. Thompson, Langmuir 2013, 29, 12969.

17. H. A. Biebuyck, C. D. Bain, G. M. Whitesides, Langmuir 1994, 10, 1825.

18. C. D. Bain, H. A. Biebuyck, G. M. Whitesides, Langmuir 1989, 5, 723.

19. I.-C. Choi, H.-G. Kang, D.-J. Lee, J.-G. Noh, Bull. Korean Chem. Soc. 2012, 33, 381.

20. J. Noh, T. Murase, K. Nakajima, H. Lee, M. Hara, J. Phys. Chem. B 2000, 104, 7411.

21. M. Tachibana, K. Yoshizawa, A. Ogawa, H. Fujimoto, R. Hoffmann, J. Phys. Chem. B 2002, 106, 12727.

22. P. Chinwangso, A. C. Jamison, T. R. Lee, Acc. Chem. Res. 2011, 44,511.

23. J. Legrand, A. Taleb, S. Gota, M.-J. Guittet, C. Petit, Langmuir 2002, 18, 4131.

24. J. Fukuda, K. Adachi, Y. Tsukahara, Y. Miwa, Chem. Lett. 2017, 46, 1330.

25. P. Bébin, R. E. Prud'homme, Chem. Mater. 2003, 15, 965.

26. R. D. L. Smith, C. P. Berlinguette, J. Am. Chem. Soc. 2016, 138, 1561.

27. I. G. Casella, M. Gatta, Anal. Chem. 2000, 72, 2969.

28. E. S. Rountree, B. D. McCarthy, T. T. Eisenhart, J. L. Dempsey, Inorg. Chem. 2014, 53, 9983.

29. O. Mabayoje, A. Shoola, B. R. Wygant, C. B. Mullins, ACS Energy Lett. 2016, 1, 195.

30. K. W. Schroder, H. Celio, L. J. Webb, K. J. Stevenson, J. Phys. Chem. C 2012, 116, 19737.

31. D. S. Hall, C. Bock, B. R. MacDougall, J. Electrochem. Soc. 2014, 161, H787.

Chapter 3

Polymeric molecular coating for oxidation resistance property

of copper surface

3.1 Introduction

Nowadays, copper has become an important material in the industrial application. Copper has excellent electrical and thermal conductivity, high ductility and easy processing. However, copper easily reacts with oxygen in air, and copper oxide is formed on the surface [1-5]. This oxide layer, composed of Cu_2O and CuO, exhibits electrical insulation, so that the electrical conductivity is impaired by intervening at the contact interface. Tamai et al. investigated the growth law of oxide layer on copper plate surface by heating temperature increased up to 300^oC [3]. From the contact resistance measurement, they determined that the effect of the oxide layer thickness on the copper plate has a little at low temperature. However, at high temperature, the oxide layer thickness increased rapidly, which greatly affected the electrical conductivity of copper.

Numerous studies on copper oxidation protection have been published and recently reviewed [6-24]. In these investigated different compounds such as azoles, amines, amino acid and their derivatives were protected the copper surface oxidation [6-12]. The copper plate protected by alkanethiols is the most investigated system of oxidation protection by long-chain organic molecules [13-21]. Laibinis and Whitesides reported that the monolayer of n-alkanethiolates on copper surface prevent the copper from air oxidation [13-17]. They demonstrated that the rates of oxidation of copper surface were decreased by increased the length of n-alkanethiolates.

Tsukahara et al. investigated the enhancement of copper plate protection by covering with PSt-SH thin layer [23-24]. From those reports, they demonstrated that the PSt-SH is efficient to provide the oxidation resistance on the copper surface. Especially at high temperature conditions, the copper surface covered by PSt-SH protected better than that covered by the alkanethiols.

In this chapter, investigation on the prevention of formation of oxide layer on the copper surface by the molecular coating with PSt-SHs different molecular weights was examined. The purpose of my study is to determine the influence of molecular weight of PSt-SHs on oxidation resistance and electrical conductivity of copper surface.

3.2 Experiment

3.2.1 Materials

Ethanol (Wako Pure Chemical, 99.5%) and THF (Wako Pure Chemical, 99.5%) were distilled and degassed by N_2 bubbling before use. Copper plate (99.98%) was purchased from Nilaco. Other reagents were used as supplied.

Thiol terminated polystyrene (PSt-SH) was synthesized by anionic polymerization of styrene with ethylene sulfide as a terminating agent under high-vacuum in a sealed reactor (Scheme 3.1). The procedure is as follows. Cyclohexane (50 mL) and s-BuLi (1M, 1.52mL) was placed in a 100mL round-bottom flask (Figure 3.1). Into the solution, styrene (5 mL, 43.6 mmol) was added through a breakable seal to allow the polymerization. After stirring at 40°C for 1h, the reaction was quenched with ethylene sulfide (0.887mL, 1.52mmol) and subsequently protonated with HCl /methanol (5 mL). The polymer was precipitated in methanol, reprecipitated twice from benzene into methanol, and freeze-dried. The polymerization conditions were shown in Table 3.1
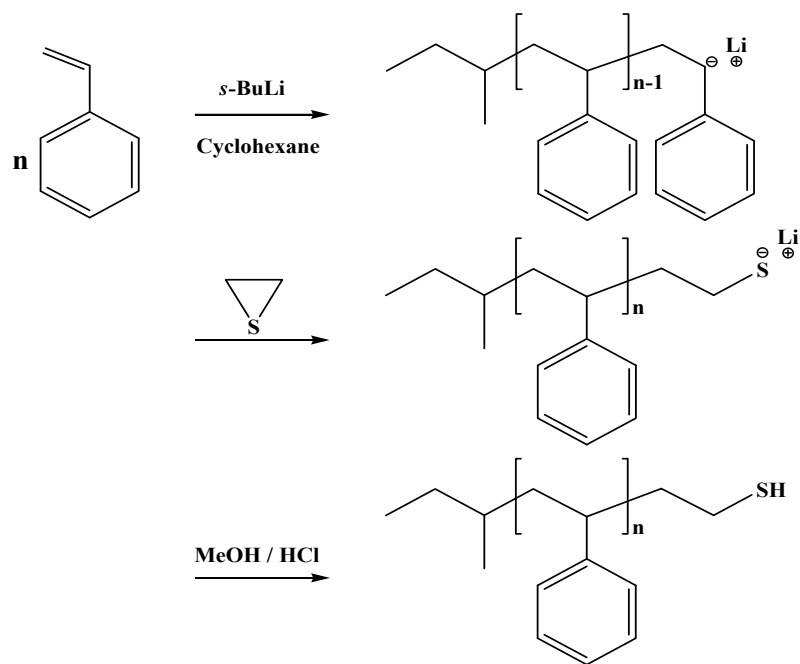
Scheme 3.1. Synthesis of thiol terminated polystyrene by living anionic polymerization.

Table 3.1. Preparation condition of thiol terminated polystyrene

Styrene	*s*-BuLi	Cyclohexane	Ethylene sulfide	MeOH/HCl	Temp	Time	Target M_n
(mmol)	(mmol)	(ml)	(mmol)	(ml)	( )	(hour)	−
96	19.9	100	19.9	5	40	1	500
43.64	1.52	50	1.52	5	40	1	3000
96	1.67	100	1.67	5	40	1	6000
96	1.25	100	1.25	5	40	1	8000
96	0.99	100	0.99	5	40	1	10000
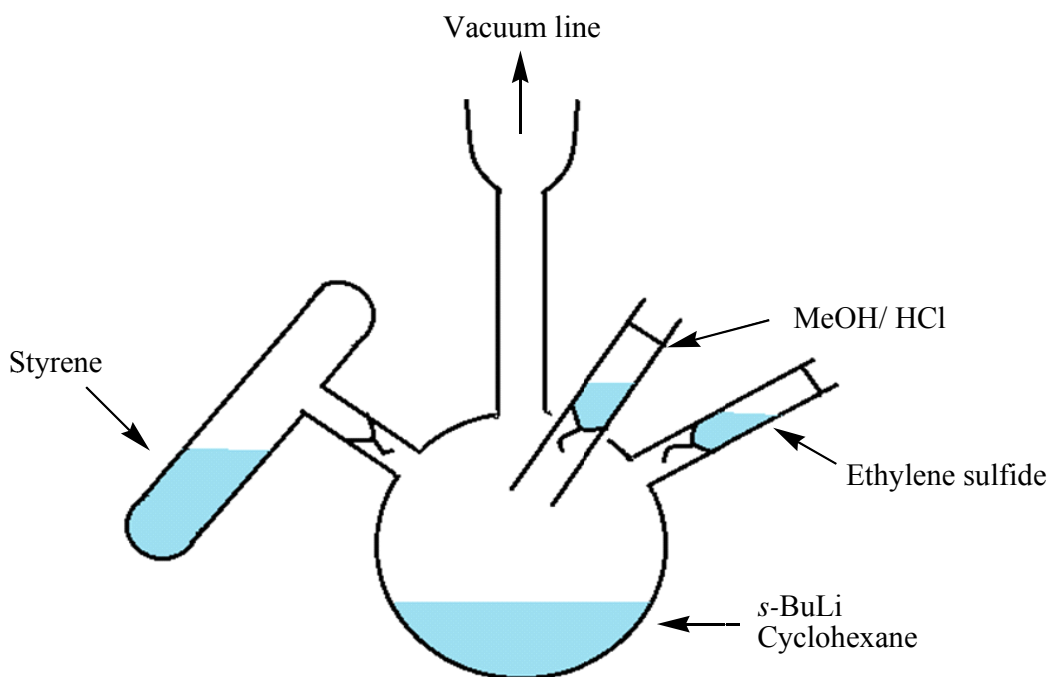
Figure 3.1. Glass reactor for synthesis of thiol terminated polystyrene.

The molecular weights of the obtained polymers were determined by gel permeation chromatography (GPC). The number-average molecular weight (Mn), weight-average molecular weight (Mw) and molecular weight distribution (Mw / Mn) of the polymers were shown in Figure 3.2-3.6 and Table 3.2.
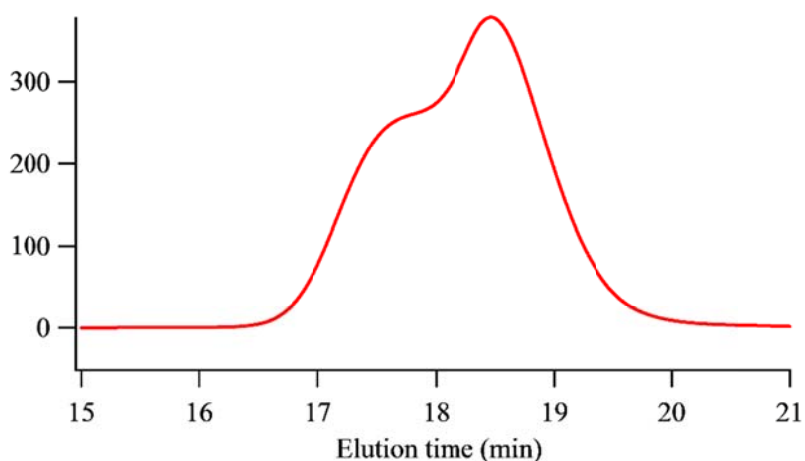

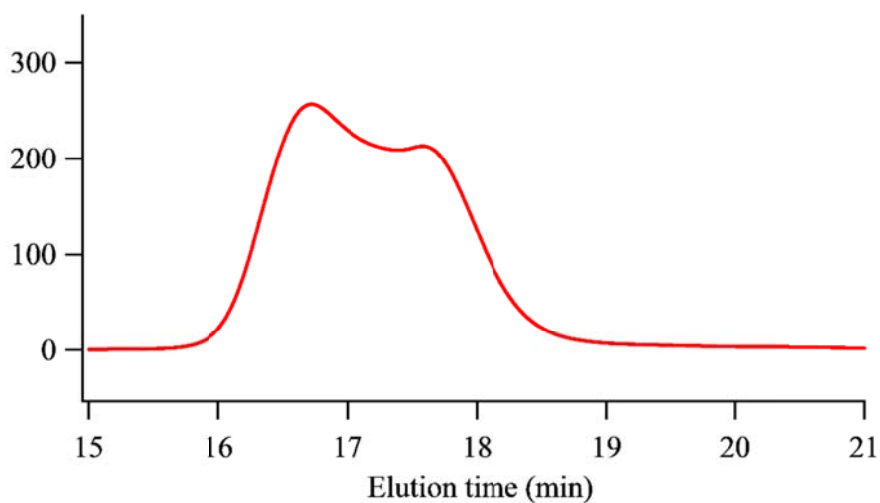**Figure 3.2.** GPC elution curve of PSt-SH850 by living anion polymerization.

Figure 3.3. GPC elution curve of PSt-SH2800 by living anion polymerization
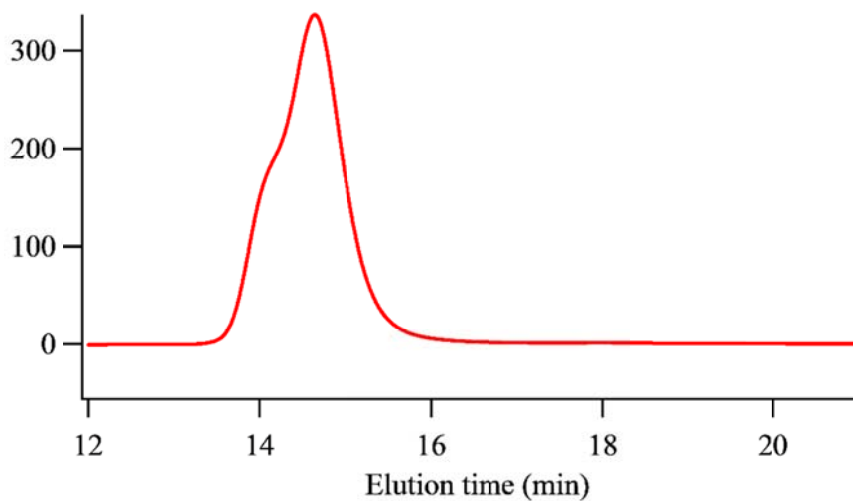
Figure 3.4. GPC elution curve of PSt-SH6800 by living anion polymerization
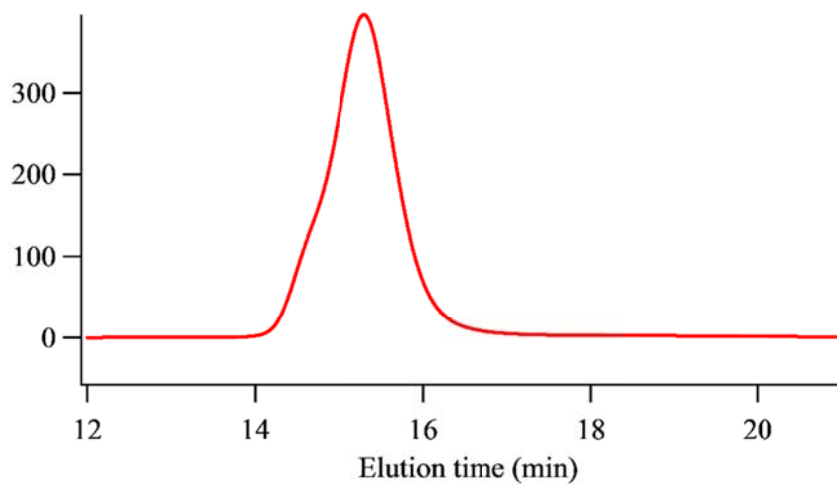
Figure 3.5. GPC elution curve of PSt-SH8600 by living anion polymerization
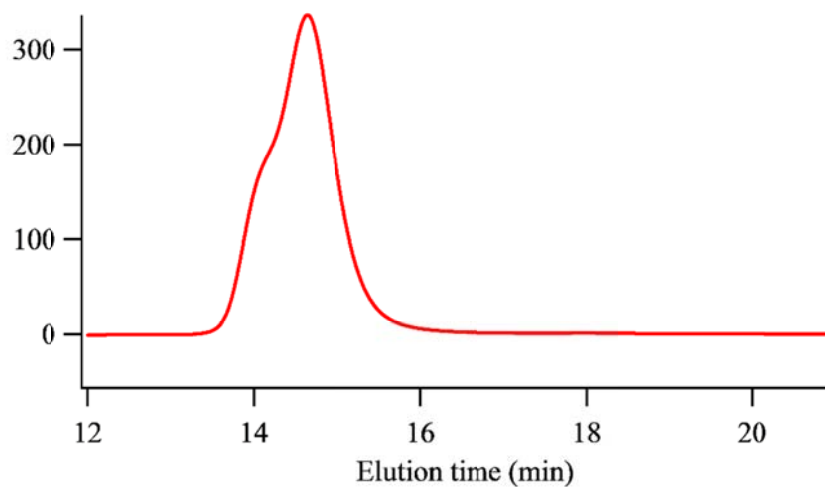
Figure 3.6. GPC elution curve of PSt-SH14700 by living anion polymerization

Table 3.2. GPC (RI) characterization of PSt-SH

Target Mn	RI			Sample name
	Mn	Mw	Mw/Mn	
500	850	1000	1.28	PSt-SH 850
3000	2800	3000	1.15	PSt-SH 2800
6000	6800	7900	1.16	PSt-SH 6800
8000	8600	9700	1.12	PSt-SH 8600
10000	14700	17100	1.16	PSt-SH 14700
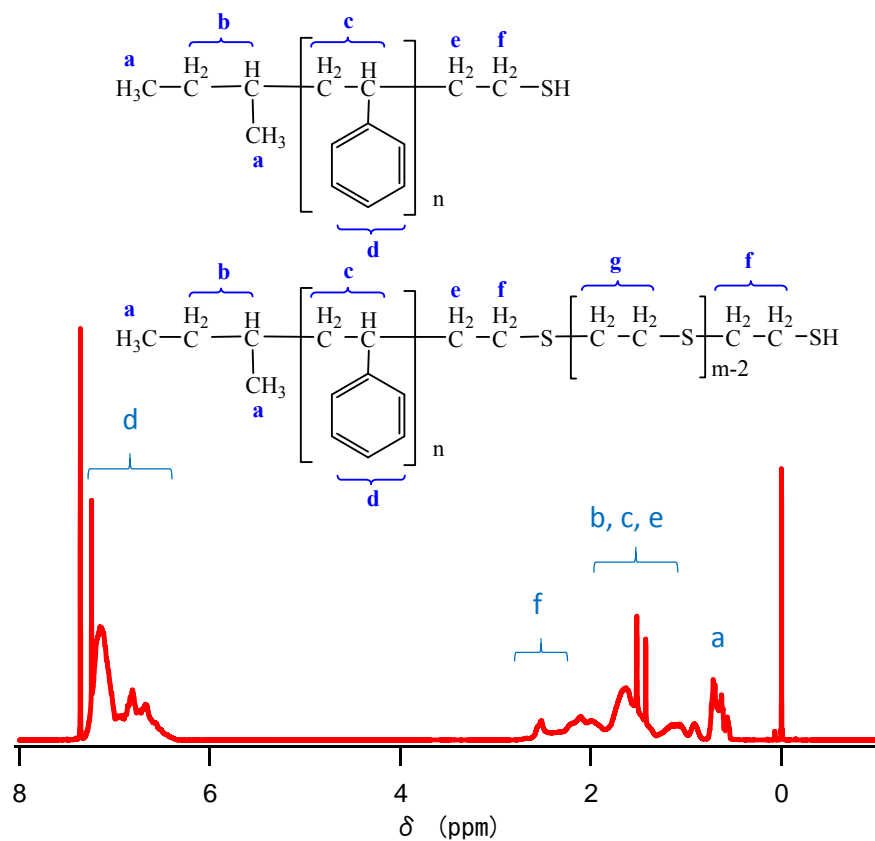
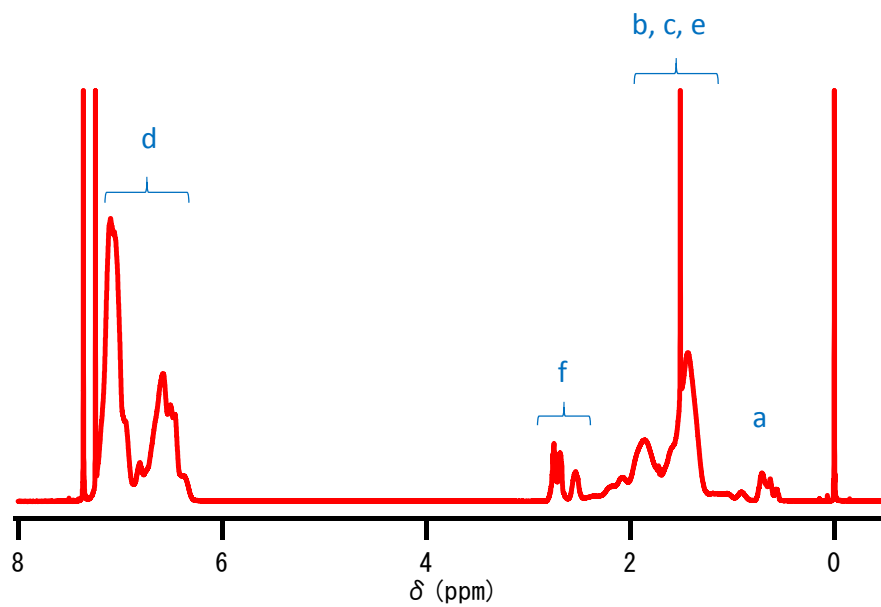**Figure 3.7.** ^{1}H- NMR spectrum of PSt-SH850 by living anion polymerization.

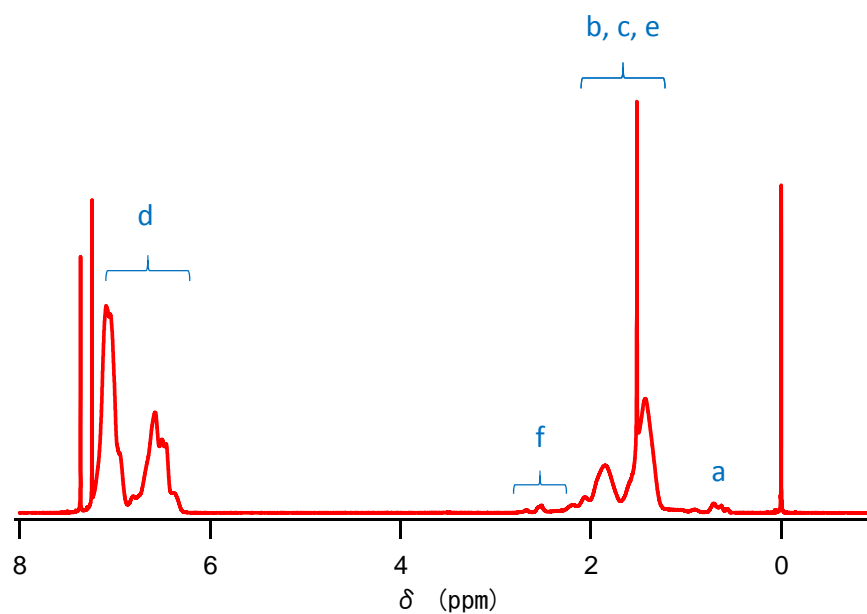**Figure 3.8.** ^{1}H-NMR spectrum of PSt-SH2800 by living anion polymerization.

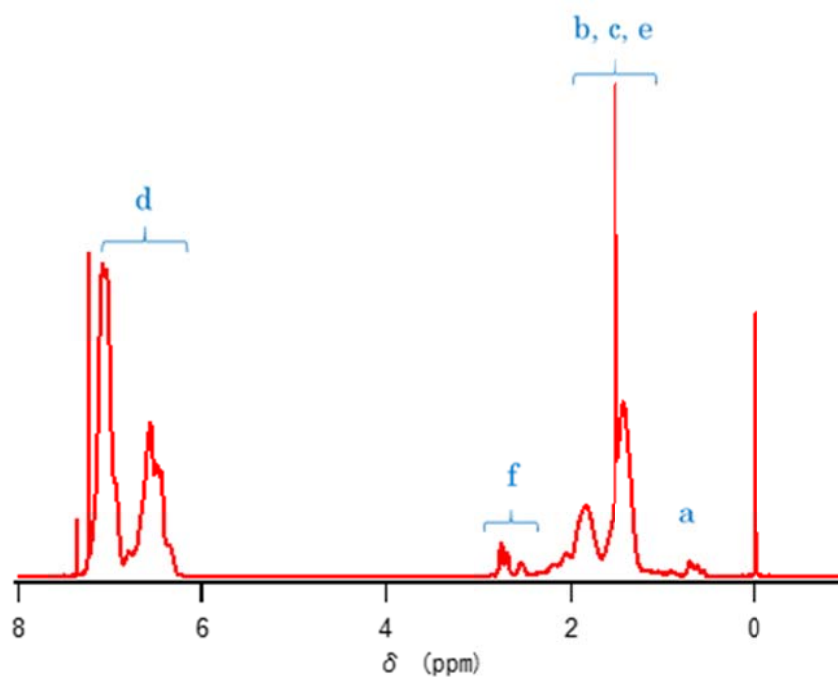**Figure 3.9.** ^{1}H-NMR spectrum of PSt-SH6800 by living anion polymerization.

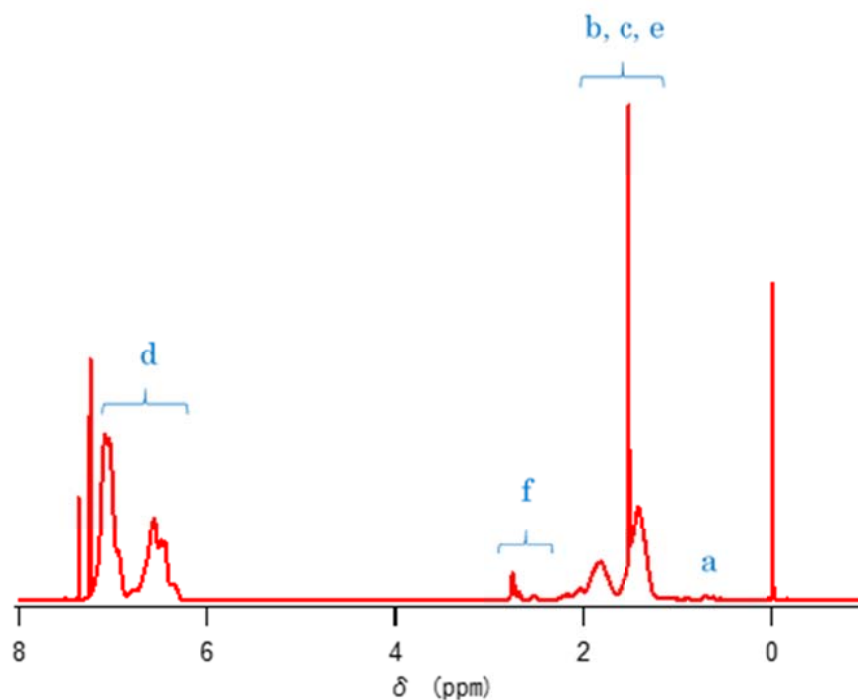**Figure 3.10.** ^{1}H-NMR spectrum of PSt-SH8600 by living anion polymerization.

Figure 3.11. ^{1}H-NMR spectrum of PSt-SH14700 by living anion polymerization.

The obtained polymers were characterized by ^{1}H-NMR (Figure 3.7-3.11). From ^{1}H-NMR spectrum of polymers obtained, the characteristic peaks the phenyl protons (d) of the terminal styrene unit was appeared at 7.2 ppm. The signals of methylene protons (f) corresponding to the terminal thiol group were observed at 2.6 ppm. On the other hand, the peak observed around 2.7 ppm to 2.8 ppm is believed to originate from the methylene group (g) adjacent to S formed at the terminal by ring-opening polymerization with excess ethylene sulfide (Scheme 3.2).
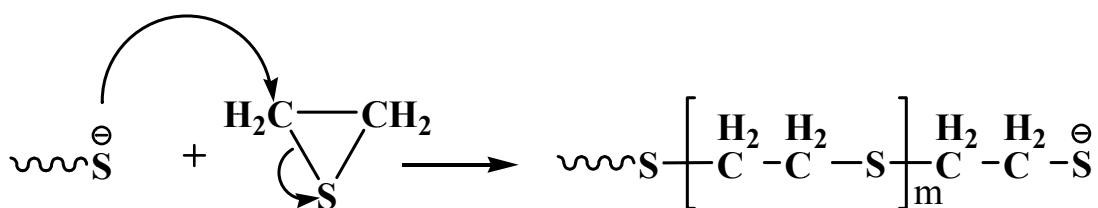
Scheme 3.2. Ring-opening polymerization of end of polystyrene by the attack of ethylene sulfide.

3.2.2 Polymeric molecular coating on copper surface with thiol terminated polystyrenes

Copper plates were polished by means of polishing paper(#1000, #2000, #4000, #8000, and #15000) and electric polishment. After polishing, the plates were washed with water, and subsequently sonicated in toluene and methanol. The plates were dried under vacuum. Before surface modification, the oxide layer of copper surface was removed by dipping of specimens in 3.7 % HCl-ethanol solution for 5 min. The plates were subsequently rinsed with distilled ethanol and dried under vacuum for 20 min. To allow the deposition of thiol terminated polystyrenes, the copper plates were dipped in THF solution of thiol terminated polystyrene for 20 hours at 35 °C. After making coatings of organic compounds on the copper surface, the specimens were rinsed THF several times to remove excessive organic compounds, and dried under vacuum for 20 min (Figure 3.12).
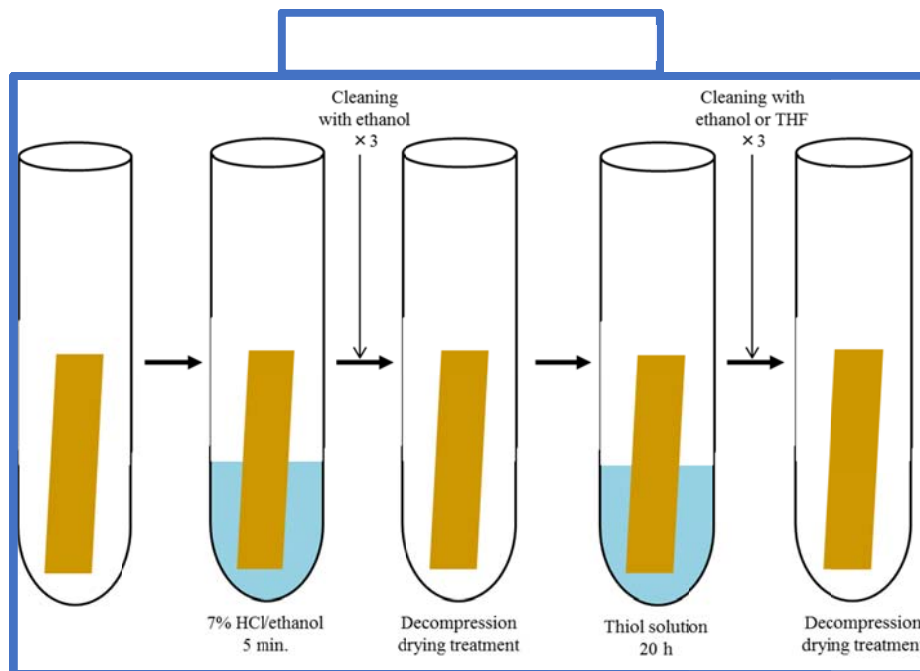

Figure 3.12. The process of formation of PSt-SH compound on copper surface.

3.2.3 Measurements

Gel permeation chromatography (GPC) was recorded on Tosoh HLC8320 equipped with a refractive index (RI) and UV detectors by using chloroform as an eluent at a flow rate of 1.0 mL/min with Tosoh G5000HHR-G3000HHR columns at 40°C. Narrowed polystyrenes were used as calibration standard. ^{1}H-NMR spectra were recorded on Bruker VB400 spectrometer in chloroform as a solvent. The chemical shifts were relative to tetramethylsilane. X-ray photoelectron spectroscopy (XPS) measurements were carried out on JEOL JPS-9010MC as shown in Figure 3.13 and Table 3.3.

Figure 3.13. X-ray photoelectron spectrometer; JPS-9010.

Table 2.3. Measurement condition of narrow scan by XPS

Voltage (kV)	10	
Emission (mA)	10	
Pass Energy (eV)	50	
Energy region (eV)	C_{1s}	290~282
	O_{1s}	538~525
	$Cu_{2p3/2}$	940~925
	Cu_{LMM}	345~325
	$S_{2p3/2}$	167~159
	Cl_{2p}	210~190
Energy step (eV)	0.1	
Number of scans	10	
Dwell time (ms)	100	

Sample specimen for scanning transmission electron microscopy (STEM) was prepared by using focused ion beam milling technique with Hitachi FB 2200 (Figure 3.14a). Pt was deposited on the samples before ion beam milling in order to introduce color contrast in the STEM images. STEM images were obtained using Hitachi HD 2700 system at the accelerating voltage of 200 kV (Figure 3.14b).

Figure 3.14. Focused Ion Beam system, Hitachi FB 2200 (a), and Scanning Transmission Electron Microscopy observation, Hitachi HD 2700 (b).

Conductivity measurements, CV, and LSV were carried out on ECstat-300 (EC Frontier, Japan) (Figure 3.15). Pt was used for counter electrode, and Ag/AgCl was used for reference electrode. CV was measured with sweeping voltage range from 200 mV to -1200 mV with a rate at 10 mV/s in 0.1M NaOH aq under N_2 flow at 50 mL/min (Figure 3.16). LSV was measured with sweeping voltage range from -200 mV to -1200 mV with a rate at 10 mV/s in 0.1M NaOH aq under N_2 flow at 50 mL/min.
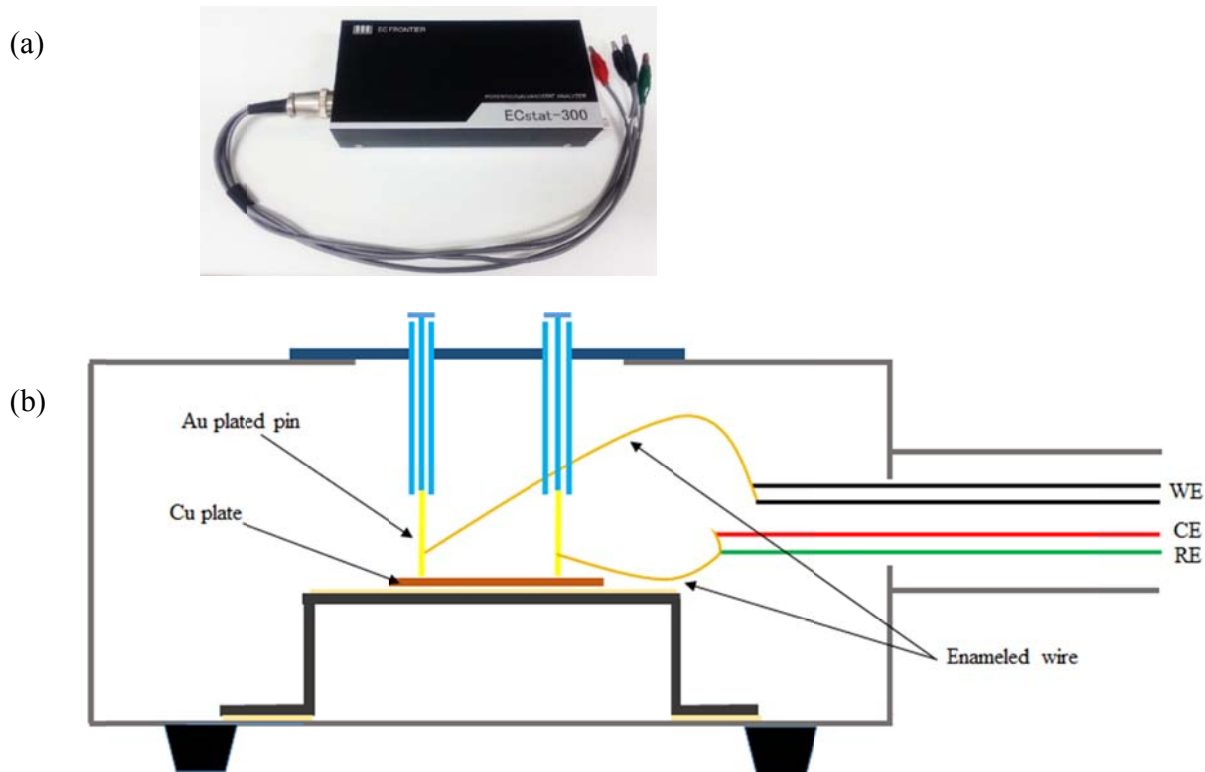
(a)

(b)

Figure 3.15. (a) Appearance of potentiostat and (b) the apparatus used to measure the contact electric resistance for the copper plate specimens.
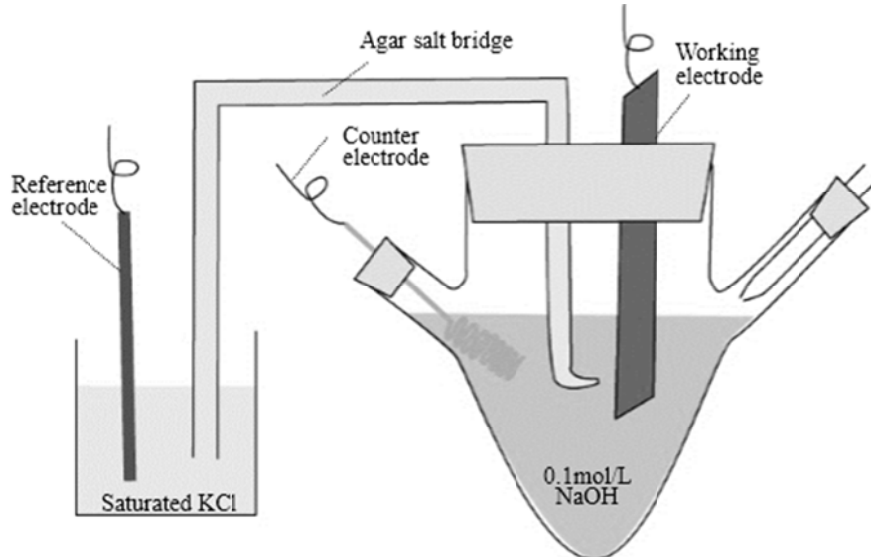

Figure 3.16. Schematic representation of the apparatus used for cyclic voltammetry.

Table 3.4. Typical experimental condition for cyclic voltammetry

Solution (mL)	Sampling interval (ms)	Filter (Hz)	Sweep rate (mV/s)	Nitrogen gas flow rate (mL/min.)
10	1000	10	10	50

3.3 Results and discussion

3.3.1. The surface protection of copper by modification with thiol terminated polystyrene

The PSt-SHs of different molecular weight were covered on the copper plate in order to determine the effect of molecular weight of polystyrene on oxidation resistance property on copper surface. Before covering, copper plates were polished by abrasive papers, buffing and electrolytic polishing for made the flat surface. The organic thin layer of PSt-SH was formed by immersion of copper plate in the polymer solutions (5×10^{-3} mol/L in THF) of different molecular weight (Figure 3.17). Depositions of the organic coatings layer on the copper plate were confirmed by XPS analysis and STEM observation.
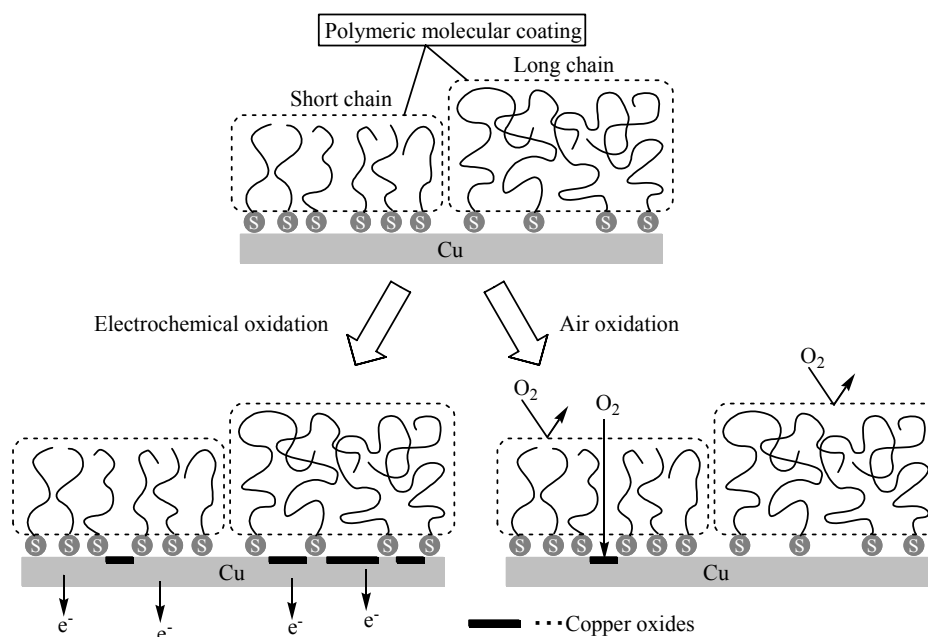
Figure 3.17. Schematic image for electrochemical and air oxidations of copper surface in the presence of polymeric molecular coatings and the effect of molecular weight of the coatings.
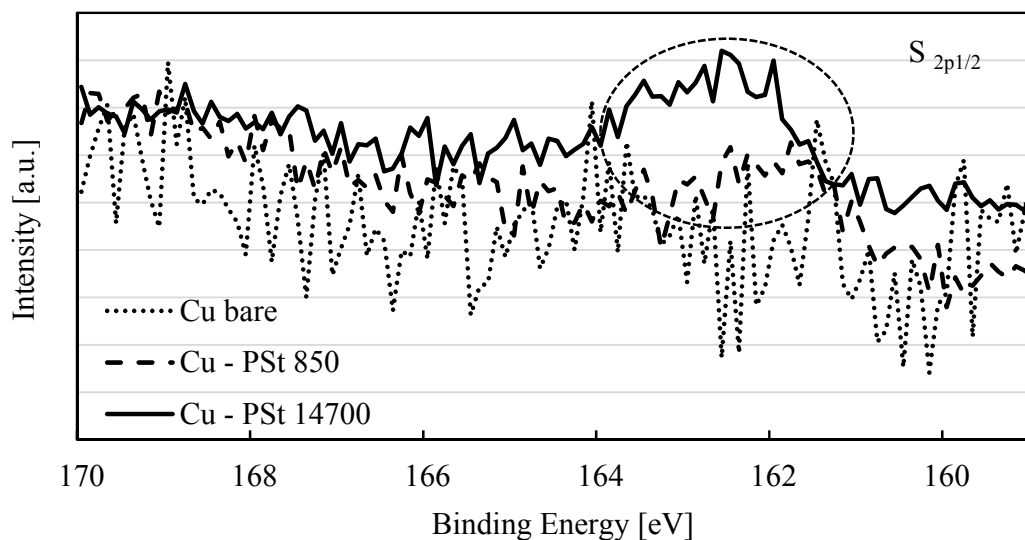

Figure 3.18. XPS core level of S $_{2p1/2}$ on copper bare and copper surfaces modified by PSt-SHs.

Figure 3.18 shows the photoelectron spectra of $S_{2p1/2}$ on copper bare and copper modified with PSt-SH different molecular weights. The analysis of the $S_{2p1/2}$ region observed the peak at the range 161 – 164 eV, which suggests that sulfur atoms of PSt-SH were adsorbed onto the copper surface, comparable with the case of copper bare showing no significant peak in this region in the spectrum. In the case of copper covered with PSt-SH14700, the peak area of the $S_{2p1/2}$ region observed bigger than the copper covered with PSt-SH850. This result suggests that the longer polymer chain was covered on copper surface better than short chain.

The surface modified copper surface was characterized by scanning transmission electron microscopy (STEM) observation. Sample specimen for STEM was prepared by using focused ion beam milling technique. Figure 3.19 shows the STEM images of copper plates before and after modification with PSt-SHs different molecular weights. The image after modification clearly shows an organic layer (bright field) in between copper substrate and surface metal layer

(Pt), whereas such layer was not observed on the sample before modification. The thickness of organic layer was observed to be ~8 nm, which is obviously smaller than the extended chain length of the polymer. Thus, the copper surface was loosely covered with the thiol terminated polymer.
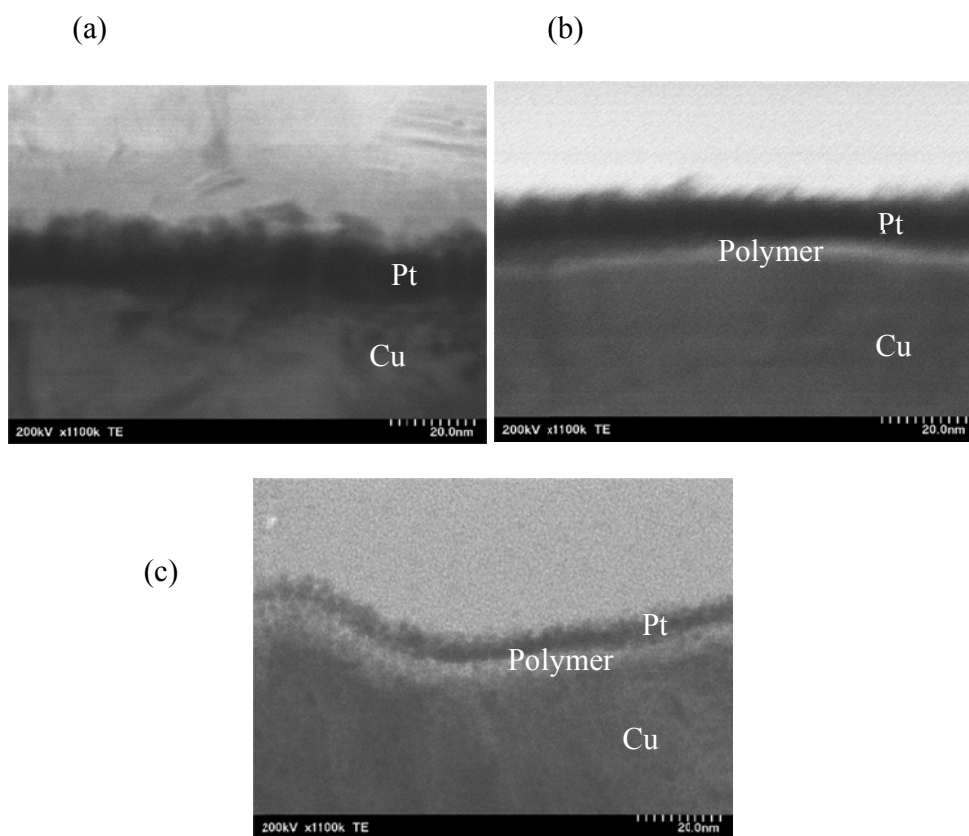
Figure 3.19. STEM images of copper surfaces, (a) without, (b) with modification with PSt-SH850 and (c) with modification with PSt-SH14700.

The surface color of the copper plates modified with PSt-SHs were changed by heat treatment. Thus the results were shown in Figure 3.20.

Figure 3.20. Influence of the heat treatment at 150°C for various heating time on the color of copper plate before and after modification with PSt-SHs

Before heating, the color of all samples was brawn. After heat treatment at 150°C, the color of the bare copper was changed from dark brawn (30 min) to yellow (2 hour) depending of time heat treatment. However, the color of copper modified with low molecular weight PSt-SH was changed slower than copper without coverage. The color of copper modified with high molecular weight PSt-SHs (8600 and 14700) were changed from brawn to dark brawn (12 hours). The changes in color of copper surfaces indicates that the thiol terminated polystyrene is efficient to provide the oxidation resistance on the copper surface. The oxidation resistance property increases with the increase of molecular weight of polymer.

3.3.2. The electrical conductivity and the oxidation property of copper

In order to determine the oxidation resistance property of copper surfaces modified with PSt-SH of different molecular weights to air oxidation, I measured surface electrical resistance of the specimens after air oxidation by heat treatments for 1 hour. The electrical resistances of the surfaces were characterized by the ECtas-300 equipment (Figure 3.21).
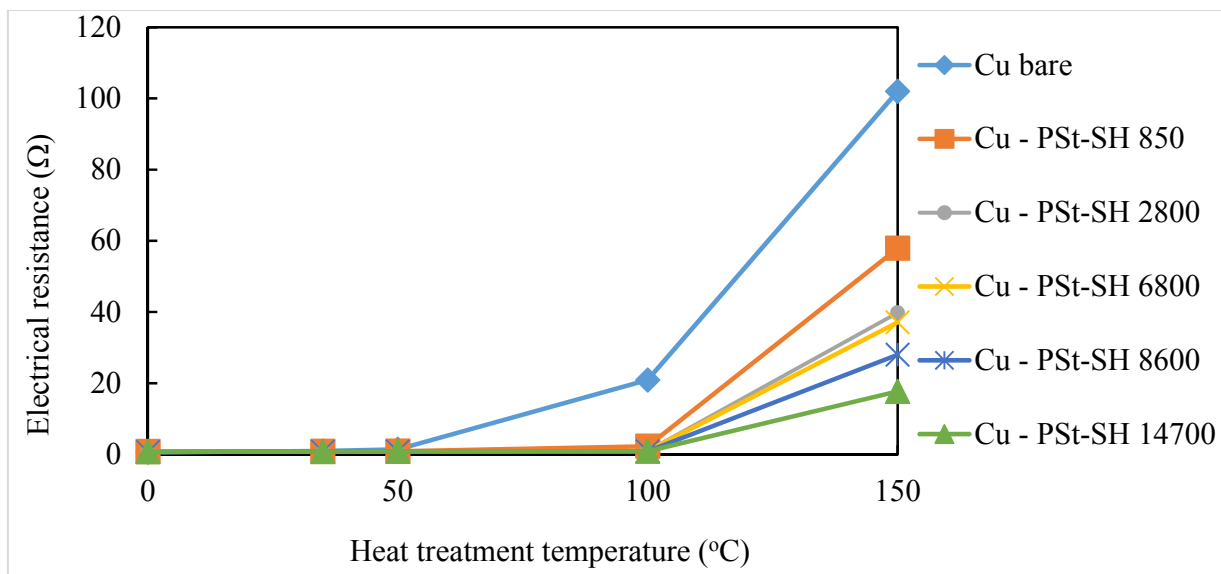

Figure 3.21. Electrical resistance of copper surface modified with PSt-SHs after heat treatment at various temperature for 1 hour.

Interestingly, all the specimens showed quite low electrical resistance before heat treatment, which might be due to the thicknesses of polymeric molecular coatings are thin enough for electrical conduction. At room temperature, the oxide layer on copper surface might be thin, which gives a little effect to the electrical resistance of the surface. The influence of the oxide layer thickness on the electrical resistance of copper was reported by Tamai and co-workers [3], who showed the small contact resistance of copper surfaces having the oxide layer less than 10 nm at room temperature.

The resistance of the copper surface without modification (Cu-bare) showed significant

increase in the electrical resistance by heat treatment at and over 100°C, which indicates the formation of copper oxide on the surface. In the case of the specimens with molecular coatings, however, the resistances of all the samples were constantly low even after heat treatment at 100°C. The electrical resistances after heat treatment at 150°C showed that the longer chain length of molecular coatings, the smaller electrical resistances. Thus, the molecular coatings of longer chain were revealed to provide higher air oxidation resistance property on the copper surfaces than that of shorter chain.

Table 3.4. The electrical conductivity of the copper and copper surface modification after heat treatment for 1 hour at various temperature.

	Heat treatment temperature (°C)				
	Before heat	**35**	**50**	**100**	**150**
Cu bare	0.587	0.957	1.420	20.900	102.0
PSt-SH850	0.808	0.850	0.895	2.280	57.9
PSt-SH2800	0.800	0.834	0.856	0.913	39.8
PSt-SH6800	0.763	0.824	0.854	0.906	37.1
PSt-SH8600	0.721	0.812	0.849	0.883	28.0
PSt-SH14700	0.710	0.781	0.844	0.867	17.7

Time dependencies of electrical resistances of copper surfaces by heat treatment at 150°C were shown in Figure 3.22.
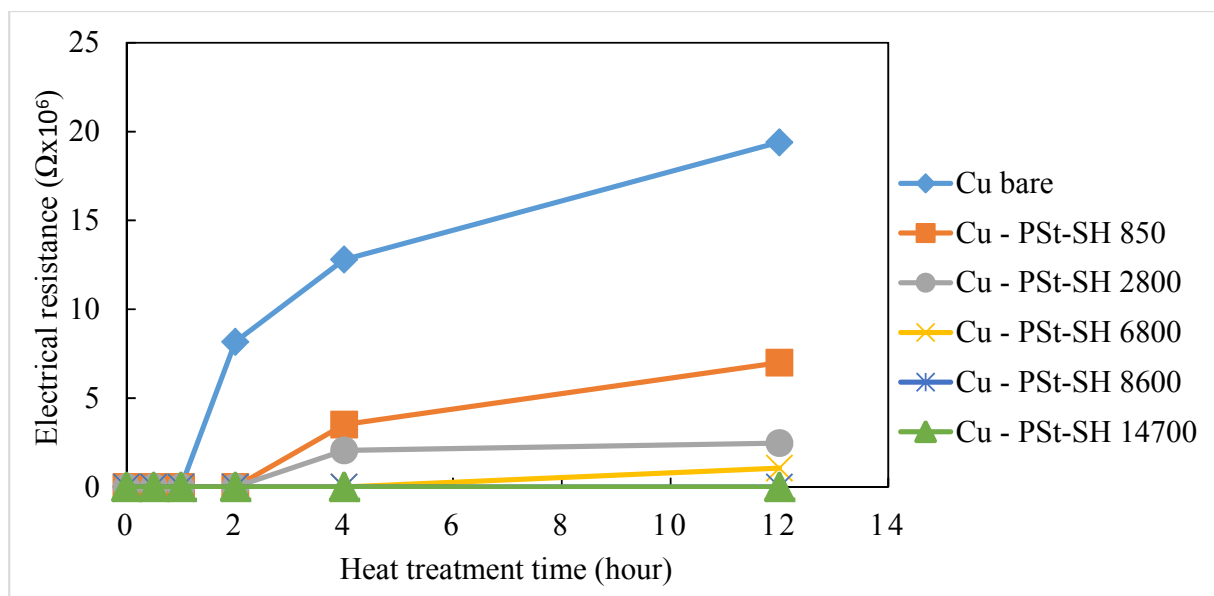
Figure 3.22. Electrical resistance of copper surface modified with PSt-SHs after heat treatment for various heat treatment time at 150°C.

The electrical resistance of copper covered with PSt-SH850 gradually increased when heat treatment time increased up to 1 hour and then rapidly increased after 2h. The electrical resistance of copper covered with PSt-SH2800 increased similarly to that with PSt-SH850 at the same heat treatment conditions. In the case of copper covered with PSt-SH6800, which kept low electrical resistance event after the heat treatment up to 4h and then the increase is accelerated after for 4h. On the other hand, the electrical resistance of copper covered with PSt-SH8600 and PSt-SH14700 increased similar at the same time and kept low electrical resistance even after the heat treated time for 12h (e.g. only 100 Ω after 12 hours heat treatment for Cu-PSt-SH14700 as shown in table 3.5). It was also observed that the molecular coatings of longer chain provided higher thermal stability on the surface than that of shorter chain.

Table 3.5. The electrical conductivity of the copper and copper surface modification after heat treatment for 1 hour at various temperature.

	Heat treatment time (hours)					
	Before heat	**0.5**	**1**	**2**	**4**	**12**
Cu bare	0.587	71.3	102	8,170,000	12,800,000	19,400,000
PSt-SH850	0.808	41.2	57.90	147	3,510,000	7,000,000
PSt-SH2800	0.800	36.8	39.80	89	2,060,000	2,470,000
PSt-SH6800	0.763	32.8	37.10	52	78	1,060,000
PSt-SH8600	0.721	20.9	28.00	31	59	122
PSt-SH14700	0.710	13.8	17.70	24	46	100

3.3.3. Electrochemical analyses

Electrical oxidation and air oxidation of the copper surfaces were quantitatively characterized by electrochemical approaches. In this research, I measured amounts of oxidation on the copper surfaces by electrochemical reduction by using linear sweep voltammetry (LSV) (Figure 3.23). Thus, the surface modified copper samples were oxidized in air by heat treatment at $150^{\circ}C$ for 1 hour, followed by electrochemically reduction by using LSV with sweeping from -200 mV to -1200 mV. After oxidation, the oxide layers formed on the Cu surfaces were the mixture of CuO and Cu_2O.

In the case of Cu bare, reductions of Cu^{2+} to Cu^+ was observed at a peak potential of ca. – 820 mV vs. Ag/AgCl. Also reduction of Cu^+ to Cu was observed at the peak potential of ca. –

1020 mV vs. Ag/AgCl. However, the significant decrease in the peak area of those peaks was observed for copper surface modified with PSt-SHs. This result indicates that the oxide formed on copper surface in the presence of the PSt-SHs was less than that on bare copper. Thus oxidation was inhibited by the molecular coating layers.
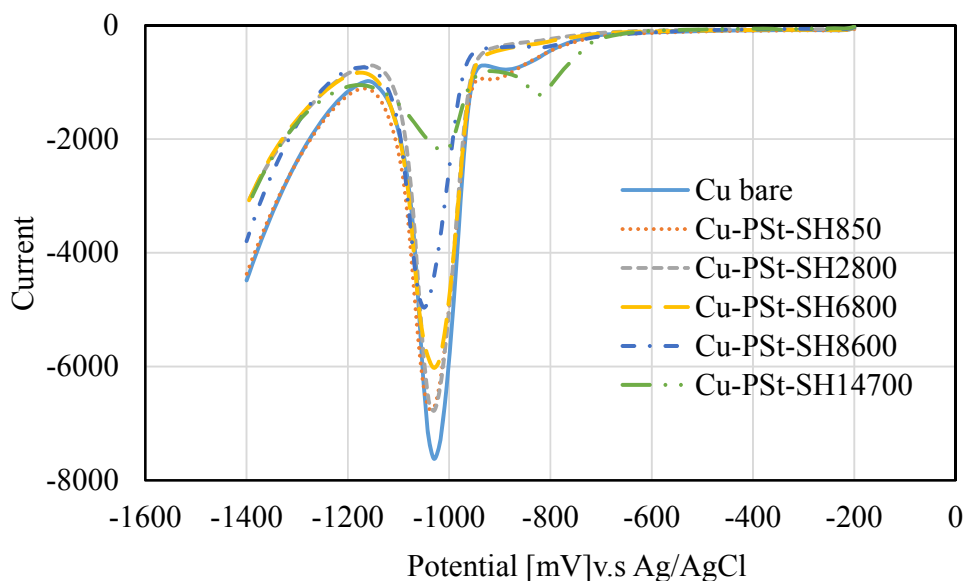

Figure 3.23. Linear sweep voltammetry of copper and copper surface modification with PSt-SHs after heated for 1 hour at 150°C. All mesurements were carried out in 0.1M acerated NaOH. Exposed electrode area was 1cm^2.

From the reduction peak area of the voltammograms, the electric charges for reduction of the oxide on the copper surfaces were calculated. The values for various samples are shown in Figure 3.24, which clearly shows the largest electrical charges for reduction for the sample without modification and the value decrease with an increase of the molecular weight of the coatings. These results indicate the higher air oxidation resistance property of the molecular coatings of longer chain, which is agreeable with the results of conductivity measurements.
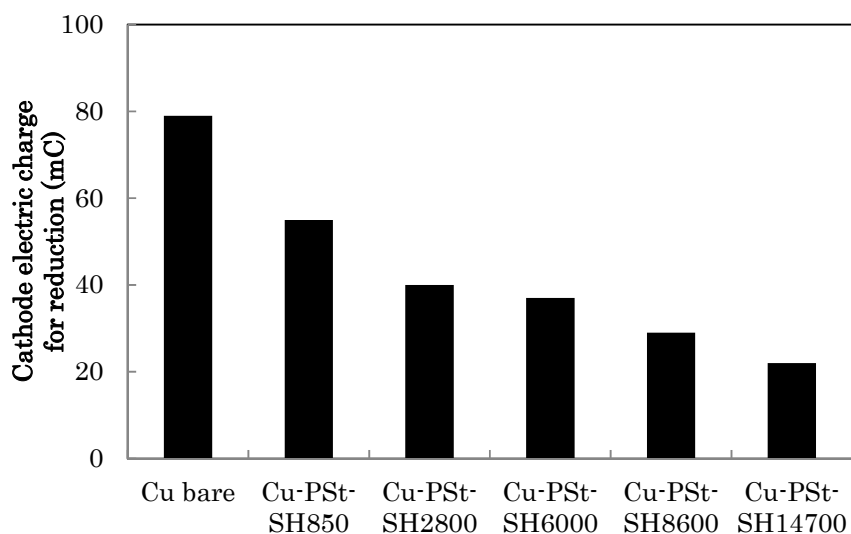
Figure 3.24. Cathode electrical charge for reduction of the copper surfaces covered with various PSt-SHs after heat treatment for 150 $^{\circ}$C for 1 hour.

In the previous research, Tsukahara et al have characterized electrochemical properties of the unoxidized metal surfaces by means of cyclic voltammetry (CV) [14, 15]. This method can be applied for quantitative evaluation of electrical oxidation properties of surface-modified metals by monitoring electrochemical oxidation and reduction. Since the peak area indicates the electrical charge for oxidation and reduction in the unmodified area left over on the metal surface, the electrical charges observed by CV should strongly relate to the surface coverage of the specimen with the molecular coatings. Here I focused on the electrochemical oxidation process to discuss about the modified surfaces. The electrical charges for oxidation observed by CV for various copper surfaces are shown in Figures 3.25 and 3.26. Also in this case, the highest electric charge was observed with the unmodified surface. Contrary to the results of LSV, the electrical charges for oxidation increase with an increase in the molecular weight of the coatings.

Therefore, it is strongly suggested that the molecular coating of shorter chain provides denser coverage on the metal surface than that of longer chain. This is the same trend for general surface grafting of polymers onto a substrate.
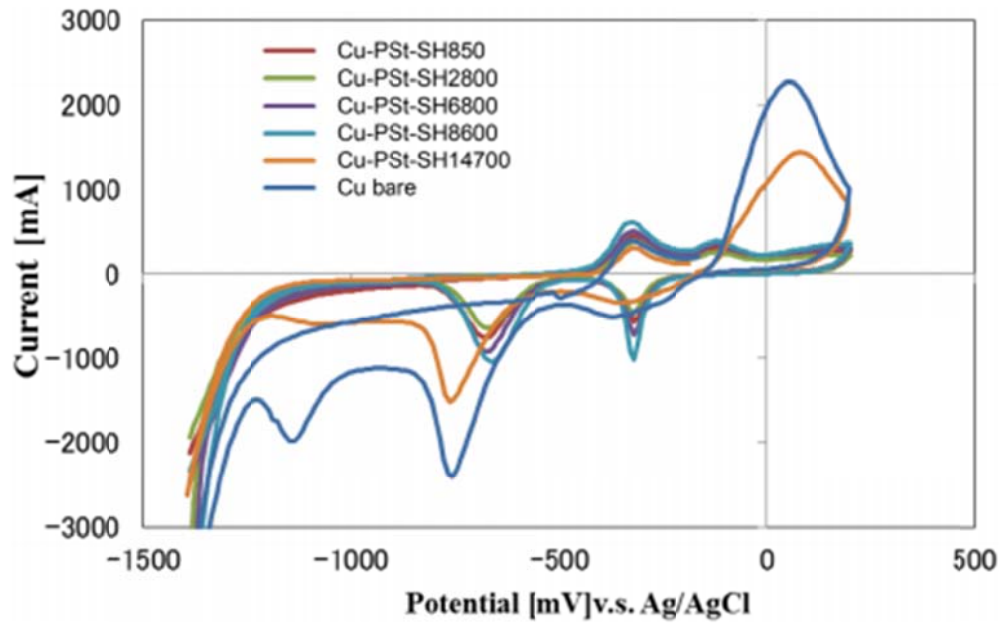

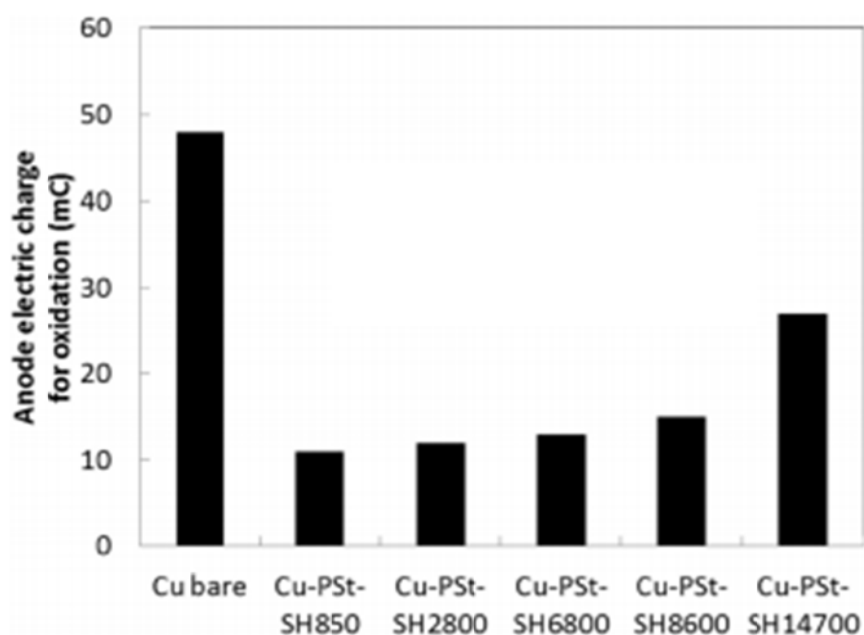**Figure 3.25.** Cyclic voltammograms of copper surfaces modified with PSt-SHs different molecular weights.

Figure 3.26. Anode electrical charge for oxidation of the copper surfaces modified with various PSt-SHs.

3.4 Summary

From the results of conductivity measurements and electrochemical characterizations of the surface modified copper specimens, the surface coverage of thiol terminated polymer on the copper surface decrease in the order of molecular weight, however oxidation resistance property is in the reverse order. Thus the polymer chain length on the metal substrate by polymeric molecular coatings is revealed to play an important role for air oxidation resistance properties of the copper surface, whereas the surface coverage produces electrochemical oxidation resistance properties.

References and Notes

1. C. G. Cruzan, H. A. Miley, *J. Appl. Phys.* **1940**, *11*, 631.

2. K. Chen, S. Song, D. Xue, *Cryst. Eng. Commun.* **2013**, *15*, 144.

3. T. Tamai, T. Kawano, *IEICE Trans. Electron.* **1994**, *10*, 1614.

4. S. Yokoyama, H. Takahashi, T. Itoh, K. Motomiya, K. Tohji, *J. Phys. Chem. Solids* **2014**, *75*, 68.

5. T. Tamai, *Nippon Gomu Kyokaishi*, **1993**, *66*, 783.

6. T. Tamai, T. Hayashi, T.Nakamura, H.Ohsaki, *IEICE technical report EMD* **1993**, *95*, 7.

7. A. Maho, J. Denayer, J. Delhalle, Z. Mekhalif, *Electorochim. Acta* **2011**, *56*, 3954.

8. P. E. Laibinis, G. M. Whitesides, *J. Am. Chem. Soc.* **1990**, *114*, 9022.

9. J. C. Love, L. A. Estroff, J. K. Kriebel, R. G. Nuzzo, G. M. Whitesides, *Chem. Rev.* **2005**, *105*, 1103.

10. F. Caprioli, F. Decker, A. G. Marriani, M. Beccari, V. D. Castro, *Phys. Chem. Chem. Phys.* **2010**, *12*, 9230.

11. F. Caprioli, A. Martinelli, D. Gazzoli, V. D. Castro, F. Decker, *J. Phys. Chem. C* **2012**, *116*, 4628.

12. T. Ikeda, K. Adachi, Y. Tsukahara, *J. MMIJ* **2016,** *132*, 39.

13. T. Ikeda, T. Takata, K. Adachi, Y. Tsukahara, *Kobunshi Ronbunshu* **2016**, *73*, 198.

14. J. Takagi, T. Ikeda, K. Adachi, Y. Tsukahara, *Kobunshi Ronbunshu* **2016**, *73*, 294.

15. K. Yamakawa, J. Takagi, H. T. Nguyen, K. Adachi, Y. Tsukahara, *Chem. Lett.* **2018**, *47*, 119.

16. M. C. Bourg, A. Badia, R. B. Lennox, *J. Phys. Chem. B.* **2000**, *104*, 6562.

17. X. Mu, A. Gao, D. Wang, P. Yang, *Langmuir.* **2015**, *31*, 2922.

18. S. Tatay, C. Barraud, M. Galbiati, P. Seneor, R. Mattana, K. Bouzehouane, C. Deranlot, E. Jacquet, A. F. Aliaga, P. Jegou, A. Fert, F. Petroff, *ACS Nano* **2012**, *6*, 8753.

19. Y. Lin, O. Ourdjini, L. Giovanelli, S. Clair, T. Faury, Y. Ksari, J. M. Themlin, L. Porte, M. Abel, *J. Phys. Chem. Solids* **2013**, *117*, 9895.

20. S. Yokoyama, H. Takahashi, T. Itoh, K. Motomiya, K. Tohji, *Appl. Surf. Sci.* **2013**, *264*, 664.

21. B. C. Worley, W. A. Ricks, M. P. Prendergast, B. W. Gregory, R. Collins, J. J. Cassimus Jr, R. G. Thompson, *Langmuir* **2013**, *29*, 12969.

22. P. Morf, F. Raimondi, H. G. Nothofer, B. Schnyder, A. Yasuda, J. M. Wessels, T. A. Jung, *Langmuir* **2006**, *22,* 658.

23. H. Huang, L. S. Penn, *Macromolecules* **2005**, *38*, 4837.

24. S. Zhang, T. Vi, K. Luo, J. T. Koberstein, *Macromolecules* **2016**, *49*, 5461.

Chapter 4
General Conclusion

This thesis describes the effect of polymer molecular coating on the oxidation properties of metal surfaces.

In chapter 1, I have clarified the importance of metals in electronic applications, particularly copper and nickel, which are indispensable materials in the electronics industry. On the other hand, this section clarified the effects of the oxide layer on the surface of the metal on the electrical conductivity of the material.

In chapter 2, I investigated the influence of polymeric molecular coating on the oxidation properties of nickel surface. In this study, nickel surface covered with PSt-SH thin layer (Mn = 2600) and 1-dodecanethiol was used to evaluate the effect of the polymer coatings. The organic layer formed on nickel surface was confirmed by XPS and CV measurement. In the results of the voltammograms, in which both the peak area of Ni-PSt2600 and Ni-D are similar size, indicate that resistance of 1-dodecanethiol and polystyrene is similar to electrical oxidation on the nickel surface.

Air oxidation resistance of the nickel surface covered with the organic coatings and thermal stability of the coatings were investigated by surface conductivity measurements of the samples by electrical conductivity measurement after heat treatment at temperature in the range of 35-270 °C for 1 h in air. The polystyrene-modified surface kept low electrical resistance even after heat treatment at 270 °C. This result indicate that PSt-SH layers protected the nickel surface from oxidation at elevated temperature in the air. The polymer layer works better than 1-dodecanethiol at high temperature over 240 ^{o}C, because of involatile long polymer chains. The oxidation resistant properties of the nickel surfaces after modification were quantitatively

characterized by LSV.

In Chapter 3, I investigated the influence of molecular weight of polymer thin films on oxidation resistance of copper surfaces. In this case, the copper surfaces were modified with thiol terminated polystyrene of different molecular weights. The organic coatings layer formation on the copper plate were confirmed by XPS analysis showing a peak derived from thiol (-SH) groups at the polymer chain end adsorbed on the copper surface. The image of STEM observation after modification clearly shows the thickness of organic layer on the copper substrate (estimates about 8nm). Thus, the copper surface was covered with the thiol-terminated polymer.

Besides that, I investigated the electrical resistance of modified copper surfaces by electrical conductivity measurement after heat treatment at the temperature from room temperature to 150°C. The electrical resistances after heat treatment at 150°C showed that the longer chain length of molecular coatings, the smaller electrical resistances. Thus, the molecular coatings of longer chain were revealed to provide higher air oxidation resistance property on the copper surfaces than that of shorter chain. CV and LSV measurements also indicate the higher air oxidation resistance property of the molecular coatings of longer chain.

Based on the above results, future work will be described.

In order to further improve the oxidation resistance of the results obtained from this study, it is considered necessary to analyze the structure of the organic thin film of PSt - SH in the future.

In chapter 2, the result was indicated the organic thin film of PSt – SH protected nickel surface better than alkanethiols. In order to improve oxidation resistance to oxygen in the air, it is important to suppress transmission of oxygen molecules. In this research, I only used PSt – SH

as a polymeric coatings. Higher oxidation resistance property is expected by the polymer coatings of low oxygen permeable polymer segments. In this research, I haven't varied the molecular weight of the coatings, thus further studies need to be made in the broader molecular weight range.

In Chapter 3, the effect of molecular weight of PSt – SH on oxidation resistance property was investigated on the ranger from 850 to 14700. From STEM images, the thickness of organic layer on copper surface was estimated about 8 nm, which was obviously smaller than the extended chain length of the polymer. This result indicates that the PSt-SH layers formed on the metal surface and protected the surface from oxidation at elevated temperature in the air. The thickness of the polymer layer should be important factor for the resistance property. Therefore, effect of polymer layer thickness will be further work in this experiment with the analysis of cross section of the samples.

On the other hand, in the electronic technology, some devices operate under high temperature conditions. Therefore, the selection of suitable polymer structures to enhance the metal's oxidation resistance under high temperature conditions is essential. Polystyrene is not a great material in its ability to inhibit air permeability as well as heat resistance. So in the future, other polymer structures could be studied to increase the oxidation resistance of metals such as polyamides, aromatic polyester, polyvinyl alcohol, ethylene-vinyl alcohol copolymer and polyacrylonitrile, etc. However, those polymers having solubility in solvents, excellent heat resistance and oxygen barrier properties are limited. In addition, it is necessary to determine the physical properties of the polymer that affect the physical properties of the coated metals. By investigating this point, the mechanism of detailed oxidation resistance will become clear, and the direction of the design of the polymer will be clarified.

List of Publications

List of papers included in this thesis:

Chapter 2

Kosuke Yamakawa, Juri Takagi, Hai Thanh Nguyen, Kaoru Adachi and Yasuhisa Tsukahara, "Oxidation resistance to nickel surfaces by molecular coating of thiol terminated polymers", Chem. Lett. 2018, 47, 119–121.

Chapter 3

Hai Thanh Nguyen, Jaeyoung Jeon, Ikeda Takuya, Kaoru Adachi, and Yasuhisa Tsukahara, "Polymeric molecular coating for oxidation resistance property of copper surface", Polymer Bulletin, 2018, DOI: 10.1007/s00289-018-2501-0

Acknowledgements

I would like to acknowledge several persons who have helped me to complete this thesis:

December 24th, 2018

NGUYEN HAI THANH